An Improved Mathematical Model to Simulate the Stock in Pulse Fired Reheating Furnaces

Alexander David Matthew

University of South Wales

A submission presented in partial fulfilment of the
requirements of the University of South Wales / Prifysgol De Cymru
for the degree of Master of Philosophy

December 2015

Abstract

The zone method of radiation analysis has been widely used in the steel industry to develop mathematical models to simulate the temperature performance of furnaces.

The zone method can provide an accurate calculation of the radiation exchanges, which are the main mode of heat transfer in the furnace. The zone method solves the radiant heat exchanges in the enclosure by splitting the furnace into a number of isothermal surface and volume zones. Applications of this method in the past have generally used a simplified representation of the furnace geometry and have not investigated the modelling of pulse fired burners.

This study aims to overcome the limitations of previous models by simulating transient furnace behaviour using long furnace models (LFM) and three-dimensional mathematical models, based on the zone method of radiation analysis. The zone model is an iterative technique that formulates a series of non linear energy balance equations.

A zone model was developed to simulate the transient thermal performance of a large continuous top and bottom fired steel re-heating furnace at Tata Steel that heats steel blooms to 1200°C at discharge. A new radiative exchange calculation program was developed called REFORM that uses ray tracing to evaluate the exchange factors between pairs of zones. REFORM also represents the furnace in a single model and allows for individual 3D blooms to be represented. The furnace contains 75 burners in total. A temperature controller and a plug-flow assumption were used to represent the opposing pulse fired burner flows.

The effect of 2D and 3D zone arrangements were investigated, the results for the 3D model was compared to a trial bloom measured data, the existing level-2 model predictions supplied by Tata steel as well as previous models. A simplified 2D LFM using a temperature controller and pulse firing technique was also used to simulate a 160 t/hr throughput rate with a short delay. The model was then validated using 74 t/hr throughput rate results. It was found that the 3D zone model has a significantly increased running time than the LFM with no obvious improvement in accuracy.

When comparing the 2D and 3D models at 160 t/hr throughput rate to measured data, the zone models' predictions did not give an exact match to the data, however, a similar temperature profile was produced. The zone models did provide a closer estimation of the

measured data than the level-2 models predictions, however, the inclusion of modelling the pulse fired behaviour of the burners provided no further improvement on the accuracy of the results.

Comparing the LFM at 74 t/hr throughput rate, to Tata Steel's level-2 model predictions, the zone model provided a similarly accurate prediction. Therefore this model was employed to examine the influence of a range of parameters on the thermal behaviour of the furnace.

All simulations were conducted with the same initial conditions with the desire to reach a discharge bloom temperature of 1200°C with good temperature uniformity.

This study has demonstrated the use of multi-dimensional mathematical zone models running under transient operating conditions that represents the entire furnace in one simulation and fully models each individual steel bloom. The REFORM program is highly flexible and can handle a range of geometries and combined with a transient zone model can be used for reheating process control.

Acknowledgements

The author would like to express their gratitude to their supervisors Dr. C.K. Tan and Professor Paul A. Roach as well as the Engineering and Physical Sciences Research Council (EPSRC) and Tata Steel UK for their financial support in this work.

Table of Contents

List of Figures

List of Tables

Nomenclature

Term	Explanation	Units
A	surface area	m^2
ai	correlation coefficients	-
ag,n	weighting coefficient in mixed grey gas model	-
bi,n	correlation coefficients	-
Cp	specific heat at constant pressure	kJ $kg^{-1}K^{-1}$
$CVnet$	caloric value of fuel	kJ kg^{-1}
dt	time-step	s
e	error	K
E	unit direction vector	-
F_{ij}	view factor	-
h	heat transfer coefficient	kW $m^{-2}K^{-1}$
H	specific enthalpy	kJ kg^{-1}
$\dot{m}i$	mass flow rate of gas zone i	kg s^{-1}
$\dot{m}in$	input mass flow rate	kg s^{-1}
$\dot{m}out$	output mass flow rate	kg s^{-1}
Pb	proportional band	K
$QGnet$	fuel energy input	kW
Qa	preheated air energy input	kW
Qwc	energy transferred to the furnace water cooling	kW
Qex	energy in exhaust gases as they leave the furnace	kW
$Qconv$	the convective heat transfer	kW
$Qrad$	the radiative heat transfer	kW
R_0	initial position vector	-
$\overline{s_i s_j}$ $\overline{s_i g_j}$ $\overline{g_i g_j}$	direct exchange area (surface-surface, surface-gas, gas-gas)	m^2
$\overrightarrow{SS_i}$ $\overrightarrow{SG_i}$ $\overrightarrow{GG_i}$	directed flux area (surface-surface, surface-gas, gas-gas)	m^2
$\overline{\boldsymbol{SS}}$ $\overline{\boldsymbol{SG}}$ $\overline{\boldsymbol{GG}}$	total exchange areas (surface-surface, surface-gas, gas-gas)	-
T	temperature	K
U	heat transfer coefficient	kW $m^{-2}K^{-1}$
Vi	volume of gas zone i	m3
ε	emissivity	-
ρ	reflectivity	-

n	cone angle	°
λ	thermal conductivity	kW $m^{-1}K^{-1}$
σ	Stefan-Boltzmann constant ($5.6687\times10_{-11}$)	kW $m^{-2}K^{-4}$
θ	circumferential angle	°

Chapter 1 Introduction

1.1 Reheating Furnaces

In the steel industry, large continuous reheating furnaces with heat inputs of up to 200 MW are employed to reheat steel slabs, blooms or billets (known as the stock or load) to a desired discharge temperature and temperature uniformity prior to subsequent hot forming or rolling. The discharge temperature of the stock ranges from 1100-1250°C with a maximum variation of 20-30°C within the stock, depending on steel composition. The heat input to these furnaces is usually supplied by a series of gas burners firing above and below the stock, which are located in a number of temperature control zones along the furnace length. Although the thermal efficiency of these furnaces has increased in recent years through the installation of regenerative or recuperative burners and improved refractory insulation, further improvements can still be achieved through better furnace control. Typically, the stock is transported through the furnace in a series of discrete steps by a pusher or walking beam mechanism so that as a hot bloom is discharged at one end a new cold bloom is introduced at the other end. For product quality reasons it is necessary to tightly control the steel discharge temperature and temperature uniformity, although this can be difficult to achieve since furnaces increasingly operate in a transient manner as a result of variations in steel composition and size, changes in stock throughput (due to the variable demands of the hot rolling mill), and the need to handle planned and unplanned production delays. Therefore, in some situations, stock of different metallurgical grades, length and cross-section may be travelling through the furnace at any one time and each of the separate pieces of steel will have different heating requirements.

Currently most furnace supervisory control systems attempt to provide the appropriate stock heating profile by regulating the furnace temperature, and hence the thermal input to the group of burners, in various “control zones” within the furnace chamber. Unfortunately it is not possible to measure stock temperatures directly, so in most control systems mathematical models are employed to predict the stock temperature and the temperature uniformity at discharge and various other positions along the furnace length. Control of the stock temperature throughout the furnace is determined by applying appropriate furnace zone temperature set-points to achieve a desired heating profile along the furnace. Existing models that have been developed (Madsen, 1994; Yan & Zhang, 2000; Anton et al., 2005),

referred to as level-2 models, mostly adopt a semi-empirical approximation where the furnace temperatures are represented by a one-dimensional temperature profile that is linearly interpolated from a small number of roof mounted thermocouples readings to estimate the source radiation to the stock. Once the rate of heat transfer to the stock has been evaluated, the heat content and temperature distribution within each individual steel piece can be calculated by finite-difference conduction models. These models are often "tuned" for a very limited range of furnace conditions by comparing the predicted stock temperatures with experimental measurements using test slabs instrumented with a number of thermocouples. Nevertheless these models have significant limitations with the radiation interchanges between the hot combustion gases and the refractory and stock surfaces being represented in a simplified manner. Since these models do not represent the actual "physics" of heat transfer processes in the furnace, their accuracy can be affected for furnace conditions that are different from those in the tests. Also, these limited thermocouple measurements cannot fully represent the temperature map over large control zones within the furnace and inconsistencies in temperature regulation can occur. Consequently the supervisory temperature control has to compromise on the inaccuracies in both measurements and modelling assumptions.

The radiation exchanges between the combustion gases and the refractory walls and stock surfaces, are represented using a simplified approach and only developed to work well using steady-state furnace operating conditions (Bhardwaj 2000; Staalman, 2004). These models are limited due to the lack of temperature measurements in the furnace which can result in inaccuracies in the predicted stock temperature. Excessive under or overheating of the blooms at discharge can occur when these model are used operating under transient conditions to their inability to respond realistically (Barr, 2003).

The EU steel industry has had to respond quickly and effectively to changing mill conditions to compete against 'lower cost' producers. As well as adapting to these different conditions, the EU steel industry has to try and minimise the reheating furnace energy consumption whilst maintaining to supply consistently heated products to the hot rolling mill. Presently, little work has been done to develop a more comprehensive model capable of simulating the dynamics of the furnace from the knowledge of the furnace heat and mass-flow balances. Existing models only aim to control the stock temperature by adjusting the thermal input to the individual furnace control zone and therefore do not achieve

optimisation of the overall furnace efficiency. As the availability of more powerful computers has increased so has the possibility to develop more rigorous mathematical models. These models can provide a better representation of the overall furnace performance by taking into account the complex furnace geometry and the furnace behaviour during periods of non-steady operation.

1.2 -Mechanisms of Heat Transfer

Heat is transferred to the refractory surfaces and stock predominantly by radiation and convection from the burner flames and combustion products. The energy that is received by the refractory surfaces will also contribute to the total energy transferred to the load, as the energy that is incident on the walls will be partially reflected towards the load. During the process of heating the stock, energy can be lost by means of conduction into the hearth and in the case of the refractory surfaces the energy can be lost to the surroundings by convection and radiation from the outside wall of the furnace chamber. Convective heat transfer is a relatively small contribution compared with radiation and it is therefore normally sufficient to make an approximate estimation of this mode of heat transfer. If a more accurate estimation of convection is required this can be achieved by isothermal physical modelling (Rhine & Tucker, 1991), or better calculations such as Computational Fluid Dynamics (CFD) techniques. Once the thermal energy is transferred to the load and refractory surfaces then conduction becomes important and can have a considerable effect on the overall furnace performance. Conduction losses are kept quite small for continuously operated furnaces operating under steady-state conditions by defining an appropriate refractory thickness. Furnaces operating under transient conditions have high storage losses due to the amount of energy the chamber must absorb to achieve thermal equilibrium when running from a cold start-up. The thickness of the load and thermal conductivity are also important due to the load interior tends to lag in temperature behind the exposed top surface. This can affect the overall temperature uniformity within the load and the overall furnace heating time. Because of the high temperatures involved in the reheating furnace, an accurate model of the thermal radiation is important for predicting overall thermal efficiency, production rates and quality of the heated product. The prediction of radiative transfer is complex due to the multidimensional and spectral nature of radiation, but for most applications concerning reheating furnaces, it can be assumed that the furnace

enclosure is grey and contains participating non-grey products of combustion, mainly carbon dioxide and water vapour. ('Grey' here means that the radiation absorbed or emitted is in constant proportion to that due to a black-body, the theoretically perfect absorber and emitter of all incident radiation (Eastop & McConkey, 1993).)

1.3 - Motivation

The motivation for the current study is to develop an improved mathematical model capable of more realistic simulation of the interchange of thermal radiation within a large-scale bloom reheating furnace equipped with top and bottom fired burners; this should have a reduced dependency on the limited temperature measurements available, whilst also being able to simulate the dynamic changes within the furnace. Existing models have also not taken into account the dynamics of the pulse firing nature of the burners. The technique of pulse firing can be investigated by incorporating the burner firing timings into a transient model.

To address the limitations of the representation of heat transfer in existing models this project will produce an improved model that incorporates more sophisticated modelling of the stock and its interactions with the upper and lower sections of the furnace. The project will build upon the experience from a number of previous research projects at the University of South Wales (previously Glamorgan), to develop an improved mathematical model to simulate radiative heat transfer in industrial steel reheating furnaces. The model devised employs the zone method of radiation analysis, originally developed by Hottel and his co-workers (Hottel & Sarofim, 1967) which has modest computational requirements as an improvement over the high computational costs of CFD, and has been used successfully to simulate the transient behaviour of gas-fired furnaces (Tucker & Lorton, 1984). An important part of the zone model is the calculation of the Radiative Exchange Areas, which are complex functions of the geometry and radiation properties of the gas and surface zones. Previously, a computer code known as RADEX, which is based on the Monte-Carlo Ray-Tracing (MCRT) technique was employed by the research team at the University to calculate these exchange areas (Correia & Ward, 2002). However this code is relatively inflexible and is not suited to calculation of the exchange areas to individual stock in top and bottom-fired furnaces. For example, an individual obstacle is represented only as a single surface zone. Moreover, it is impossible to represent multiple obstacles within a volume

zone as separate entitles, as RADEX groups all obstacle surface zones in the volume zone to form a single surface zone. These limitations greatly hinder investigation of more detailed interaction, in terms of radiation interchange. An improved radiative exchange calculator is used as a sub-model for the zone model of heat transfer within a production-scale reheating furnace, also incorporating conduction and convection. The energy balances, which are set up in the model for each zone in turn, require knowledge of the inter-zone mass flow rates for the combustion products. These can be determined off-line using an isothermal CFD procedure or by assuming a plug flow. During the transient analysis of the thermal performance of a furnace, (e.g. a system starting up from cold), the non-linear zonal energy balances must be solved simultaneously repeatedly throughout the heating period. In order for the model to work efficiently it is necessary to ensure that the iterative schemes, used to solve the equations, converge quickly. The model therefore also incorporates a module containing suitable algorithms for control of the thermal input to the burners. A pulse fired technique will be used to accurately simulate the way that each control zone's fuel input varies using existing set point temperatures.

Validating the model is vital, and so data from TATA Steel is used for this exercise as the cost of placing user specific thermocouples within the furnace would be too great. The data provided includes the measured temperatures from the top, bottom and centre of a test slab at various points along the furnace length to be assessed against as baseline experiment data. The predictions from TATA Steel's level-2 model are provided to be compared against and further validation can also be performed using experiment data for a different production rate.

1.4 - Aims and Objectives of the Thesis

The aims of this project were to achieve the accurate and detailed calculation of the radiative exchanges that occur within a reheating furnace. This will expand upon the existing ray tracing program discussed in the literature review by improving the modelling of the steel load. These radiative exchanges will then be used to predict the stock temperatures at various positions along the furnace length. The pulse firing effect of the burners will also be modelled to investigate if this will provide more accurate stock temperature calculations.

These aims were achieved through the completion of the following:

- Development of a Monte Carlo Ray Tracing Program called REFORM to calculate Total Exchange Areas (TEAs).

- Compare the results of REFORM to the existing MCRT program RADEX as well as analytical solutions.

- Development of a transient zone model of a production-scale reheating furnace, incorporating radiation, conduction and convection.

- Results and analysis of using the improved model to predict stock temperatures, with comparison against existing models that include individual top and bottom section models, and against typical plant measurements.

1.5 - Structure of the Thesis

This thesis describes the development of an improved mathematical model for predicting stock temperatures in a top and bottom pulse fired reheating furnace.

- Chapter 2 is the literature review which describes mathematical modelling followed by a detailed description of several different methods used for the calculation of radiative heat transfer in furnaces and combustion systems. The advantages and disadvantages are explained along with the application of these methods. A critical review of the published literature on the zone model is also outlined.

- Chapter 3 describes the development of the zone model incorporating the radiation sub-model REFORM (*R*adiation *E*xchange *F*ull *O*bstacle *R*ay-tracing *M*ethod), which is a Ray-tracing programme that can be adapted to a wide range of complex furnace geometry and stock arrangement encountered in steel reheating.

- Chapter 4 outlines the development of the 3D Transient Zone Model, including formulation of the energy balance equations and explains the iterative technique used to calculate the gas zone temperatures.

- Chapter 5 compares the results of REFORM to existing solutions and calculates an appropriate Ray density. The results of the 3D Transient Zone Model are compared to existing predictions and measured data.

- Chapter 6 describes the development of a transient Long Furnace Model (LFM) that includes a temperature controller and a pulse firing technique. The model is used to simulate a furnace for two different throughput rates and the predictions are compared to existing data.

- Chapter 7 draws the overall conclusions from this study with respect to the transient LFM and 3D models developed.

Chapter 2 Literature Review

2.1 - Heat Transfer Simulation Models

The reheating furnaces purpose is to heat steel slabs to the required discharge temperature with a uniform temperature distribution and to be sent to the hot-rolling mill. The furnace can operate at steady-state when the slabs have a similar heating history or at transient operation, which includes delays in operation, charging steel with varying material properties and changing stock sizes. Mathematical models make it possible to control heating over a large number of transient conditions and can ensure that this heating occurs while minimising fuel consumptions and achieving product quality requirements. The need for improved furnace and stock temperature control is well documented in the literature (Norberg, 1997; Malhotra, 2003; Anton *et al*, 2005). These models are usually written in computer languages such as C or FORTRAN. Nevertheless, physical complexity makes it difficult to predict the effects of input parameter variations on the energy consumption and/or the product quality. A way to achieve this is through the use of more accurate and sophisticated simulation models which will provide higher levels of efficiency, reliability and safety as well as being able to predict the combustion and heat transfer processes within the furnace. These models can be used to investigate the control and operation of the furnace, though it is important to validate them against experimental data. Tata steel describes an online control system for a reheating furnace (Malhotra 2003) which can be used for optimization of furnace parameters and incorporates radiative exchange and conduction sub-models. The position of the stock divides the furnace into top and bottom sections, between which there is no radiative exchange. Different firing patterns have been investigated (Barr 2003) which compares thermal excursions within allowable limits for rolling. When a furnace encounters a delay the billets have the potential of being overheated, it was found that during the delay the best option is to reduce the burner firing rates to minimum values. However, recovery from delays will result in temperature change in the discharged billets.

More recently, a study (Franci *et al*, 2008) investigates a control system where the furnace is divided into six control zones where individual zones are adjusted by the control system such that the desired slab temperature can be achieved and production delays have also been taken into consideration. A furnace control systems that implemented an online model

has also been investigated by Jang and Kim (2007) and a validation of a mathematical model for use on a pusher-type reheating furnace was carried out by Wild *et al* (2009).

The complexity of mathematical models has increased due to advances in computer technology. Computational fluid dynamics (CFD) models attempt to provide a total furnace description of the thermo physical processes involved. CFD models solve the finite-difference equations together with the conservation equations for mass and energy. These models also require the determination of thermal radiation transfer (Rhine & Tucker 1991). The radiation calculations produced with these CFD models are less accurate than that of the zone model and large CFD models require a lot of computational time.

The use of Artificial neural networks (ANN) have also been applied to furnace control applications as they are not computationally intensive. ANNs can represent the behaviour of the mathematical model over a range of conditions. The ANNs can be trained to control and optimise a furnace by using actual plant data and will act as a black box simulation tool (Chong *et al*, 1997). This type of experimental work can be deemed expensive and thus limits the procedure. However, the ANN can be trained with data obtained from a mathematical model, such as the zone model. Ward *et al* (1999) developed an ANN to simulate the transient characteristics of a simple well-stirred zone model of a gas-fired batch furnace. The ANN was able to predict the fuel consumptions, temperature difference in the load and the heating times. The results showed that the predictions of the neural network matched similarly to those of the zone model.

A genetic algorithm analysis of heat transfer was performed by Chakraborti *et al* (2000) which gave a higher level of insight into performance details of a reheating furnace.

The use of mathematical models in the steel industry has many advantages, such as, the ability to obtain results quickly, accurately and cheaply, therefore saving time and money. Many different mathematical modelling methods have been adopted over the years and the choice of method depends on what needs to be modelled.

The early development of more practical and efficient models for predicting stock temperature within reheating furnaces is reported elsewhere (Leden, 1985; Staalman, 2004), in which an effective radiative heat transfer to the stock is calculated via construction of “radiation curves” intended to represent all effects of direct and indirect heating (such as gas and wall temperatures). Each curve is the result of interpolation from measured temperature obtained from thermocouples specifically located along the roof and the side

walls of the furnace. However, these semi-empirical approaches do not directly take into account the furnace dynamic response (due to the thermal inertia of the refractory structure) nor do they take into account the energy balances within the furnace enclosure. As a result, these models are often only calibrated to work reasonably well under steady-state furnace operations (Bhardwaj, 2000; Staalman, 2004). These limitations make them less useful as a generic tool for design and optimisation of furnace operations.

On the other hand, CFD models attempt to provide a total furnace description of the thermophysical processes involved. CFD models solve the finite-difference Navier-Stokes equations. Detailed fluid dynamics, heat transfer and combustion modelling via CFD have made impressive developments (Kreuzer & Werner, 2011) and have been used successfully to analyse reheating furnaces, (Venturino & Rubini, 1995). The radiation calculations produced with these CFD models would require a great number of finite volume cells in order to produce results with reasonable accuracy like that of the zone model and the excessive computation time has hindered their use for design and control applications, especially if simulation of transient furnace operations is necessary.

2.2 - The Zone Method

Over the last two decades or so the availability of more cost effective computing power has paved the way for more sophisticated furnace models (Madsen, 1994; Yan & Zhang, 2000; Anton *et al*, 2007). The first numerical procedure employed to model engineering radiative heat transfer was the zone model and it was first introduced by Hottel and his co-workers (Hottel & Cohen, 1958). The basics of the zone model can be seen in figure 2.1

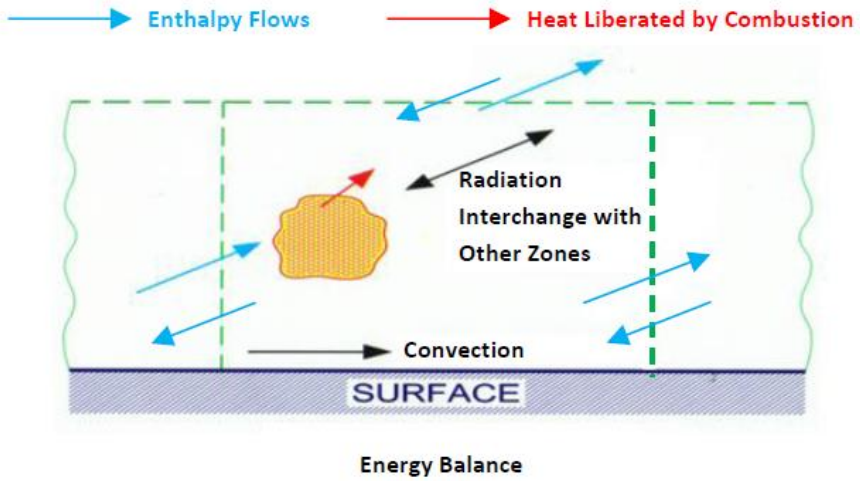

Figure 2.1 - The Zone Method

Since the zone model was first introduced, many improvements have extended the original formulation. In particular, a model described by Hottel (Hottel & Sarofim, 1967), in combination with the weighted-sum-of-grey-gases (WSGG) has been widely and successfully used to simulate the thermal performances of high temperature reheating furnaces (Tucker & Ward, 1990). The complexity of the zoning arrangement can depend on the size and geometry of the furnace. These models can be simple single gas zone or long furnace models as well as more complex multi-dimensional models.

The zone method also has a relatively modest computation time when compared to CFD. Mathematical models of this type split the furnace enclosure into a series of isothermal surface and volume zones, and energy balances are then solved for each zone, taking into account all enthalpy transport and source terms associated with the flow of combustion products and their heat release due to combustion. In the zone method, it is assumed that the temperatures and radiative properties of all surface and volume zones are uniform and that all surfaces are diffuse and grey. In these models, the other mechanisms of heat transfer (convection and conduction) are incorporated in the radiation analysis. The energy balance equations are written in terms of exchange areas known as directed flux areas between all zone pairs and need to be solved first. These exchange areas allow for the effects of surface emissivities and non-grey gas behaviour on the radiant interchange within a furnace (Hottel & Sarofim, 1967). These temperature-dependent directed flux areas can be calculated from more fundamental sets of exchange areas known as the Total Exchange

Areas (TEAs), which in turn are calculated from Direct Exchange Areas (DEAs). DEAs must be calculated: from each surface zone to every other surface zone; from each surface zone to every defined volume zone (where a volume zone contains a mixture of grey gases); from each volume zone to every other volume zone; and from each volume zone to every surface zone.

For a furnace chamber containing a grey gas and grey surfaces whose radiative properties are independent of temperature, the TEAs are themselves independent of temperature and therefore need only be calculated once for a given furnace zoning configuration. Hence, the calculation of radiation transfer in a furnace enclosure containing non-grey combustion products is simplified if the grey gas assumption can still be retained. This can be achieved by using the mixed grey gas model (Rhine & Tucker, 1991) from which the directed flux areas can be calculated by an a-weighted summation of the arrays of TEAs of a small number of grey gases and one clear gas. For the clear gas calculations only the surface to surface exchange areas need to be determined, as the clear gas has zero absorptivity. The full temperature dependence of the directed flux areas is attributed solely to the a-weighted coefficients which are generally expressed as low order polynomials of surface and volume zone temperatures.

The resultant set of simultaneous non-linear balance equations, which takes into account all modes of energy transfer, including conduction and convection, can then be solved for the gas zone temperatures and the surface temperatures or heat fluxes (direct computation instead of iterative computation for CFD). Radiation is thus treated in a global manner and is calculated using total exchange areas which are in turn derived from the geometry and radiative properties of the zones. The method was originally restricted to furnace enclosures made up of square surface zones and cubical volume zones so that this often resulted in over simplification of the furnace geometry. This restriction was relaxed by Tucker and Ward (Tucker & Ward, 1986) who used a Monte Carlo Technique to calculate the exchange areas so that they were able to model complex furnace geometries including partial shadowing of zones.

2.3 - The Monte Carlo Method

The Monte Carlo method is a statistical random sampling approach that generates a finite number of discrete bundles of energy (rays) by using random numbers. The initial position

the rays and their direction vectors are randomly but uniformly distributed. The larger the sample of rays the more accurate the heat balance calculations are.

In the case of complex geometries, the Monte Carlo method is more appropriate to generate the calculation of exchange areas as other techniques can become extremely complicated. The Monte Carlo simulates the mechanism of radiative transfer so that all important effects can be included without too much difficulty and there is no need for approximations. The zone method and Monte Carlo method have been used together as the Monte Carlo method computes the exchange factors required for the zone method calculations (Vercammen & Froment 1980) therefore reducing the computational effort in the calculations of the zone method when complex geometries are involved.

An advantage of the Monte Carlo method is that it is very flexible and able to simulate complex geometries, although the results may have some statistical errors. There computational overheads can be greater when simulating a large numbers of rays, but as computer technology has increased over the years this disadvantage has been reduced. The Monte Carlo method has been widely applied to many practical problem involving high temperature systems. For a more comprehensive review of the method and its applications to heat transfer see Howell (1997).

2.4 - Previous Exchange Area Calculation Programs

Unfortunately general software of this type does not exist since previous programs are usually dedicated to a particular furnace of fixed geometry and cannot readily be modified. In view of this limitation, Lawson and Ziesler (1996) developed a more flexible MCRT computer code called RADEX capable of calculating radiation exchange areas for a range of complex furnace geometry (Fricker *et al*, 2009; Correia & Ward, 2002; Latham *et al*, 2011) consistent with previously developed zone models. However this code is restricted in its handling of individual obstacles within furnace enclosure. For example, an individual obstacle is represented only as a single surface zone. Moreover, it is impossible to represent multiple obstacles within a volume zone as separate entitles, as RADEX groups all obstacle surface zones in the volume zone to form a single surface zone. These limitations greatly hinder investigation of more detailed interaction, in terms of radiation interchange, between individual stock and the top and bottom parts of the furnace that are separated by stock being transported by the walking-beam system along the furnace. Consequently,

Jenkins *et al* (2011a, 2011b) and others have divided the furnace into the top and bottom sections and produced two sets of radiation exchange areas separately. The net radiation heat transfer between these two furnace-sections was then calculated via simple heat balances on the imaginary boundaries joining them. Although elegant, this method compromises the direct inter-zone radiation, and hence would not be able to realistically simulate the effects of spaced gaps between the stock. This model also involved scaling the mass flow rates computed by CFD to achieve the desired stock temperature profile and discharge temperature. Other specialised commercial software that is based on the MCRT method, such as RADCad (Lucas, 1997), is also available for calculating radiation exchange areas but is restricted to only surface-to-surface radiation exchange with no intervening gas medium.

2.5 - Choice of Method

From the literature review the zone method was chosen because it is capable of accurately representing the radiation transfer within a furnace enclosure and this is the main mode of heat transfer in high temperature systems. It is evident that the ease of implementation of zone models as a tool for furnace design and control is driven largely by the availability of a flexible sub-model for calculating radiation exchange areas for a wide range of furnace geometry and stock arrangement. A Monte Carlo technique can be used to calculate the relevant exchange factors required for the zone model. Furthermore, although transient zone models have been developed previously there are still significant limitations in that previous models have always been tailored to a particular furnace so that there is a need for a flexible multi-zone model, which can be applied in a range of systems.

2.6 - Zone Model Applications

The zone method of radiation analysis has been widely applied to the mathematical modelling of furnaces. The following publications use various dimensions of zone models however some are not specified. Most use the WSGG model such as Taylor and Foster (1974) that employed the assumption to evaluate the total emissivities of luminous and non-luminous flames. The WSGG was also extended to a two phase model to include soot by Yu *et* al (2000) which was in agreement with the benchmark solution. The study aims to improve upon existing models, overcoming previous limitations.

2.6.1 - Single Gas Zone Model

A single-gas zone model is a simple example of a zone model that contains a gas of uniform temperature and several isothermal surfaces which are the load and walls the furnace (Hottel & Sarofim, 1967). The gas is assumed to be well-stirred i.e. there are no temperature gradients within the furnace. The gas temperature T_g is assumed to be equal to the exhaust temperature (Rhine & Tucker 1991). This assumption is valid in furnaces with well mixed burners have a high rate of mixing with a small flame, however this assumption is rare as the flame usually extends into the furnace chamber resulting in an exhaust temperature being lower than that of the gas temperature. Experimental data can be used to calculate a ΔT to fit the model to relate the gas zone temperature to that of the exhaust (Rhine & Tucker 1991). A single gas zone model is advantageous as the flow or heat release data are not needed and the radiation exchanges can be computed from the surface areas and partial pressures of the surface zones. Many single gas zone models have been used in applications and validated with measured data, Docherty and Tucker (1986) employed one to investigate the effect of wall emissivity on the transient performance of a reheating furnace. Varying the emissivity between 0 to 1 from a cold start up resulted in a decrease in the heat going to the blooms and small reductions in the fuel consumption.

In another study Tucker studied a single gas zone model to calculate radiation heat transfer in furnaces (Tucker 1995). A single zone model compared two WSGG models (Truelove 1976; Smith & Shen 1981), showing differences in predicted heat fluxes at higher temperatures of T_g (>1600K). Truelove (1976) concluded that zone models based on simpler WSGG models may lead to over-prediction of the heat fluxes. Single well-stirred gas models have been used to investigate furnace operating conditions (Mohammed 1997). The study investigated changes to air pre-heat, convection, fuel flow rates and excess air to evaluate the changes in the mean gas temperature and thermal efficiencies. The results showed that when increasing the air pre-heat and convective heat transfer an improvement in furnace efficiency was achieved. Increasing the fuel flow rate resulted in a decrease in furnace efficiency, but the effect of increasing the excess air resulted in a reduced mean gas temperature and thermal efficiencies.

Single gas zone models do have limitations as they are only capable of predicting the overall performance of the furnace and they ignore the non-uniformity of temperature, however

they are useful for investigating changes in furnace variables such as excess air and fuel flow rate. In order to investigate how gas and surface temperatures vary within a furnace enclosure more complex and detailed models would be required.

2.6.2 - Long Furnace Model

Long furnace models (LFM) are classified as one dimensional models that split the furnace into zones along the length (figure 2.2). Plug-flow is assumed for the combustion products where the enthalpy leaving one zone is the enthalpy input into the adjacent zone, as described by Hottel and Sarofim (Hottel & Sarofin 1967).

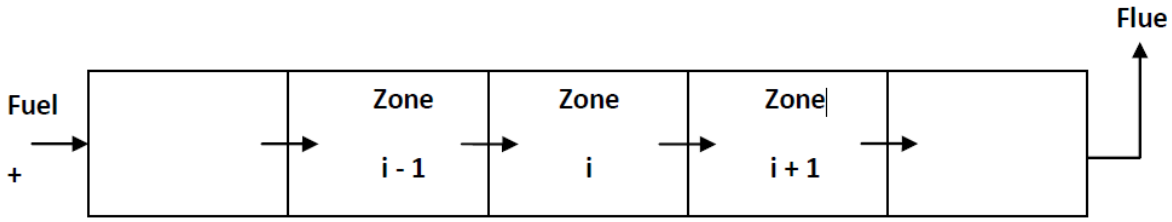

Figure 2.2 - A long furnace model

The LFM can simulate variation along the furnace length and can model the thermal and mass inputs to multiple zones by representing several burners along the length of the furnace (Rhine & Tucker 1991). Early applications of the LFM included solutions of heat conduction to the load (Fitzgerald 1969; Fitzgerald & Sheridan 1969) that showed how the zone model can be applied to predict furnace performance and also to optimise the furnace operation. The results were validated using measured data but it was found that the quantitative predictions were of limited accuracy. Fitzgerald and Sheridan (1974) extended this approach by using two different models, the first was a LFM applied to a long rectangular furnace, the second was a two dimensional model applied to a furnace with a sloped roof. The furnace geometry needed to be simplified to be able to calculate the radiative exchange factors (Hottel & Sarofin 1967), therefore, the slopping roof was modelled by a series of ‘steps’ such that all surface zones and gas zones were orthogonal. The results predicted by both models were validated using measured data. The models allowed for radiation interchange between zones and it was assumed that the furnace atmosphere was grey. The comparison of the predicted results to the measured data was

satisfactory, however, regions in the furnace where combustion was taking place showed larger differences.

Another early study carried out by Salter and Costick (1974) combined a furnace zone model with a transient conduction analysis in the stock to predict the continuous reheating furnace performance. Symmetry was assumed between the top and bottom fired chambers therefore the model only needed to simulate half the geometry. The model assumed that all surfaces were black and adiabatic and only considered radiation heat transfer within the enclosure. Assuming the furnace atmosphere was grey was found to be the main cause for the inaccuracies in the predicted results when compared to the measured data.

The application of the zone method to simulate the thermal performance of furnaces operating under non steady state conditions was first investigated by Sambi and Tucker (1983). Assuming the furnace atmosphere was non grey, the LFM predicted temperature variation inside the refractory walls and load accurately compared to measured data. This was done by building in transient conduction sub-models within the load and walls. The LFM could also predict furnace performance when running from a cold start up and could take delays during furnace operation in to account (figure 2.3).

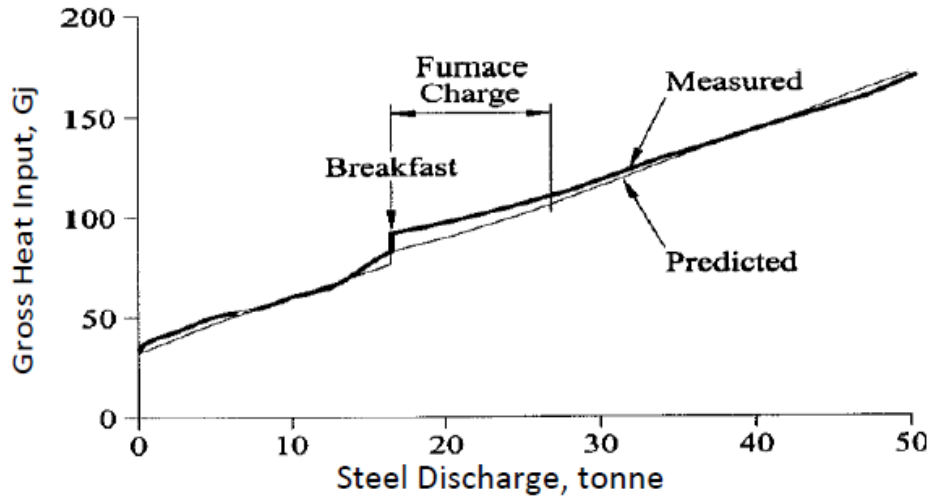

Figure 2.3 - Comparison of measured and predicted gas consumption for a Pusher reheating furnace (Sambi & Tucker 1983)

Earlier studies were restricted to rectangular furnace geometries due to the complexity involved in calculating the radiation exchange areas by numerical integration. Tucker and Ward (Tucker & Ward 1986) used the Monte-Carlo method to overcome this limitation to

determine radiation exchange areas in a LFM of a reheating furnace. This method found simplifying the furnace geometry led to significant inaccuracies in the predicted heat flux profile along the furnace length, (figure 2.4).

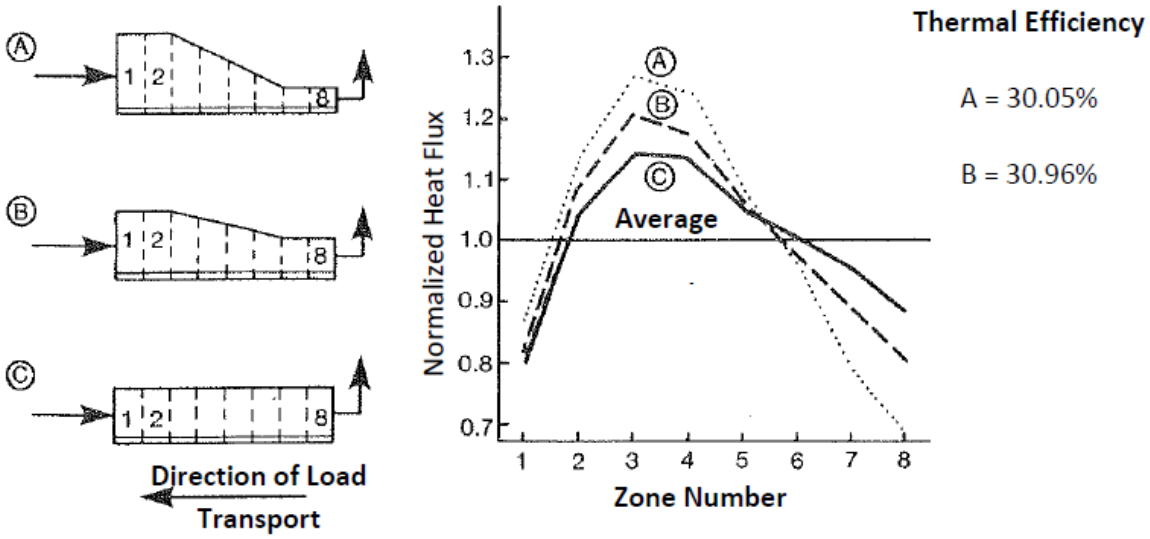

Figure 2.4 - Comparison of thermal efficiency prediction of differing geometry representations (Tucker & Ward 1986)

Tucker and Ward also compared radiative exchange areas calculated by the Monte Carlo method with those found by numerical integration. The investigation found that if enough radiation beams were simulated in the Monte Carlo method then the radiation exchange values between zone pairs that were close together were comparable to the numerical integration method. However large differences between methods was found with radiation exchange areas of distant zone pairs, but as these values are negligible in relation to the overall radiation effect the affect on the prediction was insignificant.

Tucker and Ward (1990) also went on to use the Monte Carlo technique to calculate radiation heat transfer within a natural gas fired, continuous, pusher furnace operating under non steady state conditions. The transient performance predicted by the model was comparable to measured data, which included a cold start up and production delays. The model simulated actual furnace operation by changing the fuel input of the burners in relation to the thermocouple temperature located on the furnace roof. The study also showed that further dividing the furnace geometry and hence increasing the number of gas

zones did not significantly improve the LFM accuracy. This study was later developed (Tucker, Ward & Correia 2008) to predict the thermal behaviour of a small furnace heating steel bars or billets from a cold start. The radiative heat transfer to the load was improved throughout the heating period which led to uplift in the thermal efficiency and reduced the time needed to heat the load to the required discharge temperature.

A one-dimensional zone model was applied to describe the thermal processes in a long roller-hearth furnace (Wu *et al* 2007). Heat transfer from the rollers to the slabs was ignored for simplicity and the slabs were assumed to be symmetrically heated. The results showed similarity in the temperature of the gas, surface and slabs. As the slabs moved through the furnace the temperature difference between the outer surfaces and centre of the slab gradually reduced.

2.6.3 - Multi-Dimensional Models

The furnace can also be split in to two and three-dimensions (Rhine & Tucker 1991), figure 2.5 shows an example of how a furnace chamber can be split into a two-dimensional zone model.

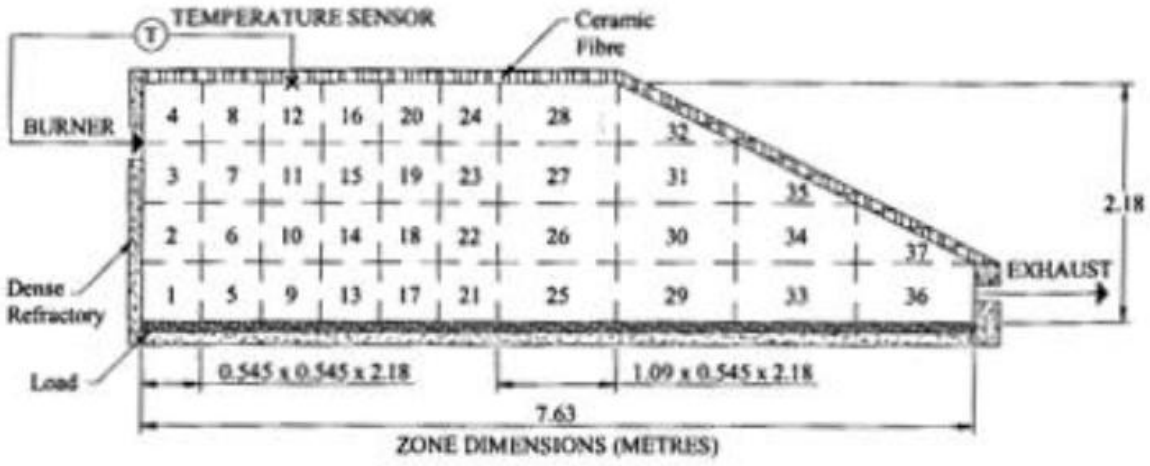

Figure 2.5 - Zoning of a steel reheating furnace (Correia, Ward & Sousa 2000)

Using multidimensional zone models often results in significant computational overheads, with increased processing time and required input data. A two-dimensional mathematical model of a cylindrical combustion chamber was investigated by Steward and Tennankore (1979) which combines the zone method with a finite difference solution for the flow

equations. The furnace enclosure was divided by using a fine zone grid and the radiation transfers were calculated by the zone model using the Monte Carlo technique. The model took into account the conservation of energy equations for every zone within the furnace chamber and the combustion products were represented by a mixed grey gas model of 3 grey gases and 1 clear gas. The predictions differed from that of the measured data with the likely reason being due to the simplifications introduced in the combustion sub-models.

A steady state zone model of a large cylindrical rotary kiln was simulated by Jenkins and Moles (1981) where predictions were compared to that of measured data. The model used a mixed grey gas model with 2 grey and 1 clear gases to simulate the non-grey behaviour of the combustion products including soot formation. The exchange factors were adjusted to allow for the varying concentration of the absorbing gas and the heat release rates were derived by integration. The model demonstrated good comparison with the measured and predicted data apart from the zones near the source of the burner flame. Goutiere *et al* (1999) used a two-dimensional model to compare different real-gas models including the WSGG model. The study found that the WSGG model provided a rapid and qualitative description of the radiative heat transfer for a multidimensional model.

A study by Omori *et al* (1991) investigated a three-dimensional model to simulate the interaction between fluid flow, combustion and radiation occurring in a steel heating furnace under steady state conditions. The zone model using the Monte Carlo technique was applied to calculate the radiative exchange area and a CFD package was used to determine the heat release and flow patterns. The combustion gases were assumed to be grey, the thermal properties of the surfaces were assumed to isothermal and the stock has a fixed temperature throughout the calculation. The results obtained from the model were compared with experimental data (Omori 1990) and the predicted results of the gas, surface and load temperatures followed the expected trends.

Steward and Guruz (1974) detail a three-dimensional model that simulates the heat transfer in a large boiler. A mixed grey gas model with 3 grey gases and clear, which included soot, was used to represent the combustion products. The model was validated with data available in an operating plant, however uncertainties in the input data, such as the flow, heat release and radiative properties of the atmosphere affected the predictions. A study to demonstrate the equivalency of a WSGG model against a quadrature of spectral results was performed by Modest (1991). The model incorporated the Monte-Carlo technique and

showed that the zone model has a time saving of up to 95% over that of the quadrature of spectral results method. A three-dimensional furnace zone model was employed by Coelho (2001) where it was found that the WSGG model can sometimes lead to unsatisfactorily accurate results. However, a study by Trivic (2004) again using a three-dimensional model found that the WSGG assumption found that agreement with other models such as ray-tracing was very good.

The transient operation of a furnace heating aerospace components has been simulated using multi-dimensional zone models by Sousa *et al* (1996; 1997). As the geometry of the furnace was relatively simple it was decided to represent the top part of the furnace as a single gas zone model and the bottom part of the furnace as an LFM. The model allowed for opposing facing alternatively fired burners with plug flow of the combustion products assumed. The computer program, RADEX (Lawson 1991) which is based on the Monte-Carlo technique was used to calculate the relevant exchange areas. The model was validated using measured data for both load temperatures and fuel consumptions. The model was in good comparison for both fuel consumptions and the stock temperature time histories for both cold and hot start-up conditions. Errors in assessing the heat losses through the walls led to inaccuracies in the predicted fuel consumptions near the end of the cycle.

Correia *et al* (1999) investigated the use of a two-dimensional zoning arrangement of a gas-fired metal reheating furnace and compared the results with that of a LFM. It was found that when comparing the two-dimensional model with that of a LFM that representing the furnace using a LFM may not always be appropriate. A range of LFM and two-dimensional models to predict the thermal behaviour of a continuously operated reheating furnace was also investigated (Correia, Ward & Sousa 2002). The study showed that the predictions of each of the types of zone models can be vastly different. The LFM was found to over predict the load temperature at discharge, the temperature difference in the steel and also the thermal efficiency. The results suggest that the use of a more complex two-dimensional model would be more appropriate when investigating changes in the design and control of the furnace. A study into the effect of varying the two-dimensional zoning has also been investigated (Correia, Ward & Sousa 2000) where it was found that a finer zoning arrangement near the burners is important to take into account the recirculation of the combustion products in this region.

2.7 - Limitations of Previous Models

The literature describes a number of methods for improving zone method applications and while the zone model approach has been widely used, it has often been limited to simplistic models such as a LFM where the combustion products have been represented as a plug flow along the furnace length. The majority of applications consider steady-state operation and only a few publications considering transient operation have been investigated. Most models also assume the stock to be a flat “lump” which can cause inaccuracies in the heat flux calculations to the load.

Since the development of large continuous steel reheating furnaces with full 3D modelling of the stock in a top and bottom pulse fired reheating furnace has not been displayed in the past, the present study will extend the work of zone modelling from existing literature such that:

- An improved radiation sub-model that can represent the entire furnace in the same simulation will be developed with the steel load being represented as individual 3D objects. These results will be validated against analytical solutions and an optimal ray density will be investigated.

- Three-dimensional transient models of a large reheating furnace at Tata Steel will be developed and validated using measured data supplied by Tata Steel as well as existing model predictions.

- Equivalent LFM’s will be developed and compared to measured data and predictions from both the Tata Steel and the three-dimensional model.

- Application of the LFM will be investigated, looking into different operating conditions, such as throughput rate and delays. A plug-flow assumption will be incorporated into this model such that a temperature controller method can be investigated. The controller will calculate the proportion of the burners maximum fuel input rate needed for the stock to reach the required temperature in a particular control zone.

- A pulse fired burner firing pattern will also be investigated to determine whether this more realistic modelling of the furnace operation will affect the accuracy of the results.

Chapter 3 - The Zone Method of Radiation Analysis

Following the computational and other benefits of the zone method (shown in Chapter 2.2 of the literature review), as an improvement on the high processing costs of CFD, the zone method was selected for this project. In view of the limitations in RADEX and other commercially available software discussed in the literature review, this project initially focuses on the development of an improved MCRT program called REFORM (*R*adiation *E*xchange *F*ull *O*bstacle *R*ay-tracing *M*ethod), to determine the radiation exchange areas in a large top and bottom fired walking-beam long-product furnace. REFORM has also been designed to allow accurate modelling of complete radiation interchange between individual stock faces and the surrounding zones in the top and bottom parts of the furnace using advanced ray tracing techniques. Therefore the directionality of the radiation interchange between the top and bottom parts of the furnace is preserved.

3.1 - Development of Radiation Sub Model (REFORM)

The Zone method of radiation analysis originally introduced by Hottel and Cohen (Hottel & Cohen, 1958) and then further developed by Hottel and Sarofin (Hottel & Sarofin, 1967) is one of the most comprehensive methods available for calculating radiative heat transfer within a furnace enclosure. The Zone Method requires the furnace enclosure to be divided into a number of isothermal volume and surface zones. Energy balances are then formulated for each zone taking in to account all energy exchanges. When using a transient model the initial surface temperatures are specified and the gas volume zone energy balances are solved to calculate each gas zone temperatures and heat fluxes to each surface zone. The temperature distributions within the stock and refractory walls can then be updated using finite difference conduction. This process is then repeated for a number of time steps to model the transient temperature profile of the furnace (Rhine & Tucker, 1991). Radiative interchange terms between zones within the enclosure called ‘exchange areas’ need to be calculated that take into account partial absorptions of non-grey combustion products.

3.2 - Monte-Carlo Random Sampling Method

The Direct Exchange Area (DEA) between a pair of zones is derived from the view factor which is only dependant on the relative orientation of the surface and volume zones as well as the intervening grey gas absorption coefficients. The view factor F_{ij} of zone j from zone i can be interpreted as the fraction of the radiation emitted from zone *i* which is directly incident upon zone *j*. The radiation exchange between two diffuse surfaces i and j is demonstrated in figure 3.1, where the radiation beams (rays) are emitted in straight lines where not all the radiation leaving surface *i* will arrive at surface *j*.

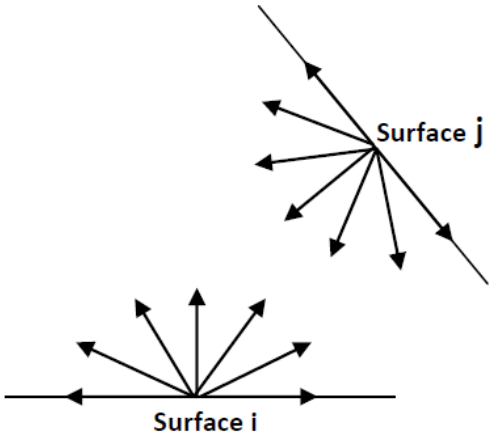

Figure 3.1 - Radiation exchange between two surfaces

To calculate view factors analytically, a complex double integral calculation can be performed for each zone pair (Incropera & De Witt, 1990). The zone pairs *i* and *j* are sub-divided into small cubic volume zones and square surface elements and then the exchange areas between each of the individual elements are summed. In order to achieve accurate results small element size is required. However, this method presents a major computational overhead, especially for furnaces complex geometries and a large number of zones.

A collection of cubic volumes and square surfaces can be used to represent the geometry of a furnace enclosure (figure 3.2).

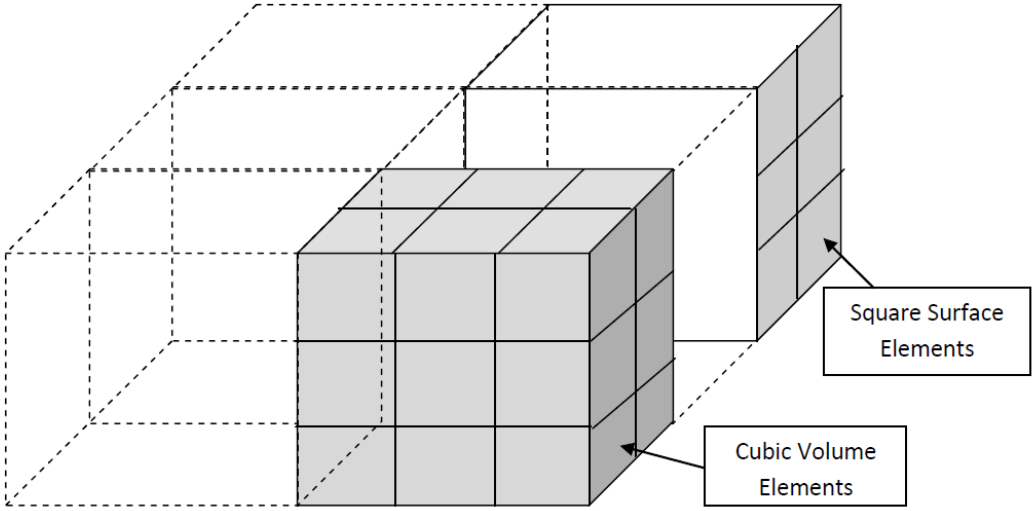

Figure 3.2 - Example of the subdivision of a furnace into surface and volume zones

REFORM employs the Monte Carlo method, which is a repeated random sampling statistical method, and which has been employed for simplifying view factor calculations (Howell, 1997). The method involves the generation of a large random sample, which is then investigated to find the statistical likelihood of some outcome. As radiation can be physically represented as directed bundles of radiant energy (rays) which travel in straight lines from any given zone, this application is a good candidate for the Monte Carlo method. A large sample of rays can be generated and each individual ray is assigned properties based on a uniform random number generator. These properties are the initial position of the ray and its unit direction vector, and are used to calculate through which zones a given ray will pass and which surface zone it will eventually reach. The fraction of the total rays fired from a zone *i* that impact another zone *j* is then calculated to give the view factor, F_{ij}:

$$F_{ij} = \frac{Number\ of\ rays\ emitted\ by\ zone\ i\ that\ intercepts\ zone\ j}{Total\ number\ of\ rays\ emitted\ from\ zone\ i}$$

As well as being dependent on the geometrical configuration of the zones, the view factors are also reliant on the gas absorptivity inside the furnace. This is because the further radiation travels before it reaches its destination surface zone, the more it will be absorbed by the intervening gas.

The view factors are represented in matrix form (Rhine & Tucker, 1991). Once the view factor between every zone pair has been calculated they are arranged into 4 matrices for

the surface-to-surface, surface-to-volume, volume-to-surface and volume-to-volume view factors. Each matrix is of the form *i* x *j*, where *i* is the sending zone. For surface sending matrices, each element is multiplied by the sending surface area, A_i, to obtain the DEA matrices:

$A_iF_{ij} = \overline{s_i s_j}$ (surface-to-surface) or $\overline{s_i g_j}$ (surface-to-volume).

Similarly, for volume-to-volume and volume-to-surface exchange areas, each element is multiplied by $4kV_i$, where *k* is the particular gas absorption coefficient and V_i is the volume of the sending volume zone, to obtain the DEA matrices:

$4kV_iF_{ij} = \overline{g_i s_j}$ (volume-to-surface) or $\overline{g_i g_j}$ (volume-to-volume).

3.3 - REFORM

When using REFORM to create a model of a furnace enclosure, the user defines: furnace geometry; obstacles; gas absorptivity; surface emissivity. The furnace geometry and obstacles are input as by the user as a set of 3D coordinates to form a fine grid that define the vertices of each object. From this information, REFORM can calculate all necessary information for each zone, including whether a given face is a solid wall or an inter-zone boundary plane. The knowledge of the volume zone connectivity is also established and is useful when calculating the inter-zone exchange of thermal energy (due to the flow of products of combustion) in the furnace. The model employs a small number of grey gases and a clear gas to represent the radiative properties of the products of combustion within the furnace. Every zone is assumed to be filled by the same mixture of these gases i.e. uniform radiative properties were imposed throughout the furnace enclosure. The gas absorptivity for each grey gas is accounted for by specifying its absorption coefficient. The surface emissivity is required for taking into account the radiation reflected from the all surface zones in the furnace. Output is given in matrix form and initially selected from view factor values, DEA values or both; if the user selects to continue to TEA calculations, those values are also subsequently output.

3.4 - Vector Geometry for Ray-Tracing Calculations

In determining the surface zone hit by a ray, the trajectory of the ray is used to calculate all surface zones (furnace wall and obstacle faces) that lie along its path. Of these surface zones, the surface zone that is nearest to the source of the ray is the one which the ray actually strikes. The view factor calculated in this way must take into account any attenuation due to absorption by gas according to the distance travelled by the ray prior to striking the surface zone. The source locations of the rays to be traced are chosen randomly from either a solid surface zone or from within a volume zone.

For a ray emanating from a surface zone, for example, a randomly chosen initial position vector R_0 that lies on the surface zone and a unit direction vector *E* must be selected (Rhine & Tucker, 1991; Walker, 2010). To define the hemispherical direction in which the ray is fired, relative to the surface zone, two angles must be chosen randomly - the cone angle, ***n***, from 0° to 90° and the circumferential angle, ϑ, from 0° to 360° shown in figure 3.3.

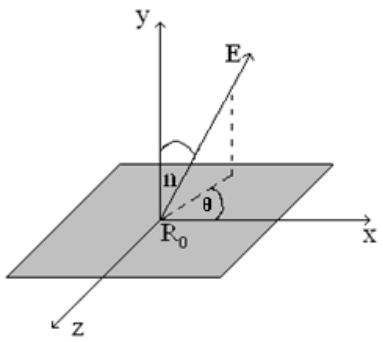

Figure 3.3 - Example of a Ray showing the initial position and unit direction vector split into the *x*, *y* and *z* components

For a ray emanating from a position within a volume zone, the directional vector must be chosen randomly such that the cone angle is assigned from 0° to 180° instead, to allow for spherical direction.

Rays are traced, from each surface and volume zone, using their initial position and direction vector information to calculate each position *R* at which a given ray intersects the plane of every surface zone defined within the furnace. The general equation of a plane, $Ax + By + Cz = D$, is employed (Zeeb & Burns, 1999), where the terms *A, B* and *C* are

coefficients within an *xyz* Cartesian coordinate system and *D* is the distance from the origin to the plane.

The position of the ray *R* on any plane is given by $R = R_0 + Et$, where *t* is the distance the ray travels to the plane and can be calculated; hence *R* can be found for each surface zone potentially intersected by the ray. A test is performed to find the surface zone which the ray actually strikes by simply using coordinate information (described in Chapter 3.5). This enables view factors to be calculated for all pairs of zones.

It should be noted that view factors to volume zones are non-zero in general unless for clear gas. To calculate view factors to individual volume zones, the distance the ray travels through each volume zone needs to be determined. The amount of radiation absorbed by a particular volume zone is the difference between the amount entering and the amount leaving, as determined using the following equation (Rhine & Tucker, 1991), where $t(n)$ is the length of the ray in gas zone *n*:

$$F_{z-n} = e^{-k*t(n)} - e^{-k*t(n+1)}$$

Any radiation remaining is then absorbed by the first surface zone that the ray intersects.

3.5 - Ray-Tracing and the Modelling of Obstacles

The approach taken by REFORM to modelling obstacles (*i.e.* the stock being heated in the furnace) allows them to be located, correctly, on a walking beam elevated midway within the furnace. Unlike previous Monte Carlo ray-tracing programs mentioned in the literature review, such as RADEX (Lawson 1991), REFORM models the obstacles modelled individually, rather than being grouped together as a single aggregated object, allowing rays to pass between objects and to travel on to a more distant face of the furnace wall.

Each obstacle that lies on the walking beam in the furnace enclosure is formed as a right rectangular prism, and orientated such that its six rectangular faces are respectively parallel to the walls of the furnace. This convenient structure and orientation simplifies the furnace model and the ray-tracing calculations. The boundary vertices of the face of an obstacle are given simply by the maximum and minimum *x*-, *y*- and *z*-coordinates of the face, within the coordinate system for which the furnace walls are regarded as being orthogonal. Hence, if a ray is found to pass into a zone containing one or more obstacles (as indicated in figure 3.4),

it is only necessary to check the nearest of these maximum and minimum coordinates of any obstacle face to determine whether the path of the ray intersects that face.

In the case of multiple intersections between the trajectory of the ray and the surface zones of obstacles and a wall of the furnace (again illustrated in figure 3.4), the solid face nearest the source of the ray is determined to be the face that the ray actually strikes. Again attenuation of the rays is treated in the same way as described in the previous section .

3.6 - Improving Efficiency

While the potential intersections of a ray with surface and volume zones can be determined by exhaustive consideration of every zone in the furnace, the structure of the furnace, and the partitioning of it into zones, allow for reductions in the calculations actually required.

3.6.1 - Bounding Box

First, a bounding volume method (Ding *et al*, 2004) is employed by REFORM, which enables the consideration only of surface zones within the volume zones with which the trajectory of the ray intersects. In figure 3.4 (indicating only a cross section of a furnace enclosure, for ease of explanation) the ray potentially passes through four of the six bounding volume zones and potentially intersects two faces of the steel load as well as a surface zone on the furnace roof before reaching the bounds of the furnace enclosure. Unnecessary checks for intersections with surface zones in the shaded zones are eliminated. (Clearly it is the 'leftmost' face of the intersected obstacle, as depicted in the cross section, that is intersected first.)

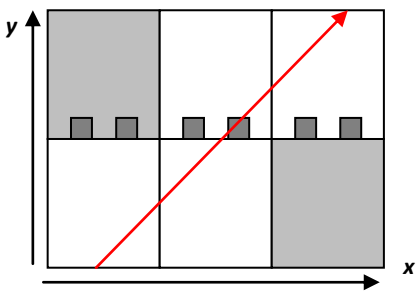

Figure 3.4 - Example of a Ray passing through volume zones in a cross section of a furnace enclosure

3.6.2 - Voxel Traversal

Second, by considering the zones in the order in which the trajectory of the ray passes through them, further unnecessary calculations can be avoided. It is more likely that a ray will intersect a surface zone in a closer volume zone than one further away.

The voxel traversal method (Amanatides & Woo, 1987) determines the next volume zone that the ray would pass through given the unit direction vector of the ray. From a current zone, 3 out of the 6 faces of the bounding volume zone are checked for intersection depending on whether the *x*, *y* and *z* directional components of the ray are positive or negative. If the roof face of the bounding volume zone is intersected then the zone above is checked next, or if the face in the positive *x* direction is intersected then the volume zone in the positive *x* direction is checked next, and so on. If a ray intersects an edge then the next volume zone checked is the one connected to the current volume zone only by this edge. Likewise, if a corner is intersected then the volume zone that shares this corner with the current volume zone only is investigated next. A flow chart for REFORM is detailed in figure 3.5.

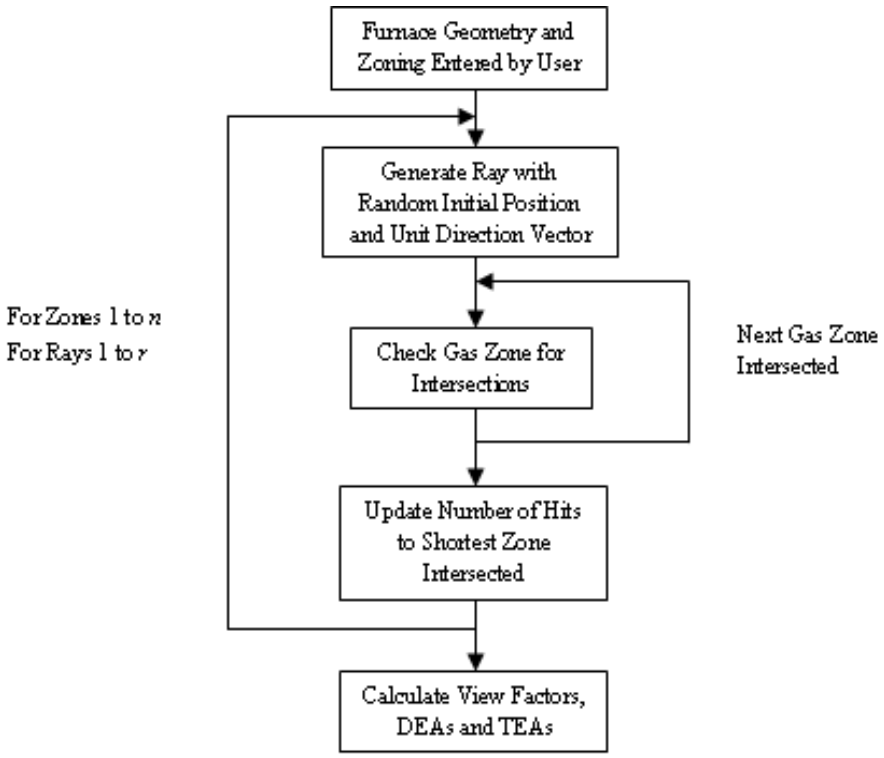

Figure 3.5 - Flow chart of REFORM

3.7 - Smoothing Direct Exchange Areas

The summation rules are used to check the calculation of the DEAs, however the DEAs calculated will contain statistical errors that prevent the summation rules from being met. If these errors are above a specific bound, then heat balance equations will not converge to a solution. Hence it is typical to perform *smoothing* of the DEAs to ensure that the summation rule is met prior to calculating the TEAs. Smoothing DEAs is a process of taking the approximate DEA values and adjusting them to satisfy the conservation and symmetry rules (Lawson, 1995). The conservation rules are

$$\sum \overline{s_i s_j} + \overline{s_i g_j} = A_i$$

$$\sum \overline{g_i s_j} + \overline{g_i g_j} = 4kV_i$$

The symmetry rules are given as

$$\overline{s_i s_j} = \overline{s_j s_i}$$
$$\overline{s_i g_j} = \overline{g_j s_i}$$
$$\overline{g_i g_j} = \overline{g_j g_i}$$

These equations can be obtained by performing an energy balance on a zone in thermal equilibrium with its surroundings. The summation rules are used to check the calculation of the direct exchange areas and if they are not satisfied then the calculated energy balance at each zone will either have an error or no solution will be found. If the conservation equation is satisfied but not the symmetry rule then the DEAs can be smoothed to achieve symmetry. Smoothing is applied by setting the modified $s_i s_j$ and $s_j s_i$ to the average of the two. Conservation is achieved by finding the average error (D_i) in DEAs for each zone, calculated by:

$$D_i = \frac{A_i - \sum s_i s_j}{m_i}$$

Where m_i is the number of non-zero DEAs for surface zone *i*. The value of D_i is added to each DEA in row *i*. This causes the matrix to no longer be symmetric, and therefore the formula for correcting symmetry is used again. However, this then results in the conservation rule being broken. A new average error D_i is calculated and the whole process is iterated until the appropriate level of accuracy of convergence is achieved.

3.8 - Calculating Total Exchange Areas

The DEAs only consider incident radiation at a surface; however, in an actual furnace radiation reflected can be taken into account by the total exchange areas. TEAs can be determined from the smoothed DEAs using explicit matrix formulae. The formulae required were derived by consideration of the radiative energy balance on each zone (Noble, 1975). The calculation of surface-to-surface ($\overline{\boldsymbol{SS}}$), surface-to-volume ($\overline{\boldsymbol{SG}}$), and volume-to-volume ($\overline{\boldsymbol{GG}}$) TEA matrices are performed using the following formulae:

$$\overline{\boldsymbol{SS}} = \boldsymbol{\varepsilon AI.R.}\overline{\boldsymbol{ss}}\boldsymbol{.\varepsilon I}$$

$$\overline{\boldsymbol{SG}} = \boldsymbol{\varepsilon AI.R.}\overline{\boldsymbol{sg}}$$

$$\overline{\boldsymbol{GG}} = \boldsymbol{gs.\rho I.R.}\overline{\boldsymbol{sg}} + \overline{\boldsymbol{gg}}$$

Where $\boldsymbol{R} = [\boldsymbol{AI} - \boldsymbol{ss.}\ \boldsymbol{\rho I}]^{-1}$ and $\boldsymbol{\varepsilon}$ is the emissivity of a surface zone and $\boldsymbol{\rho}$ is the reflexivity ($\boldsymbol{\rho} = 1 - \boldsymbol{\varepsilon}$).

When using a grey gas model, the calculation of the total exchange areas only has to be performed once for a given geometry, fixed surface emissivity and grey gas attenuation coefficient as they are independent of temperature.

3.9 - Summary

This chapter has described the development of the program REFORM that calculates the radiative exchanges within the furnace enclosure using the zone method of radiation analysis. The next chapter will describe the development of the transient zone model and will explain how REFORM's calculations fit into the model.

Chapter 4 Development of the 3D Transient Zone Model

4.1 - Zone Model

The zone method of radiation analysis has been widely used for the prediction of heat transfer in furnaces since its development (Hottel & Cohen, 1958). Zone models can range from simple Long Furnace Models (LFMs) to complex multi-dimensional models. The arrangement of the zones that subdivide the furnace depends on the furnace geometry and other features of the furnace such as burner and roof positions.

As mentioned in the previous chapter, REFORM allows for both the top and bottom sections of the furnace to be modelled at the same time, therefore the transient zone model must also be modelled in the same way. The improvement in predictive accuracy of this technique with no assumptions of the exchanges between the two sections of the furnace will be investigated.

The zone models developed simulate the transient thermal energy transfer within the top and bottom pulse fired re-heating furnace during a cold start-up. A transient zone model is capable of predicting stock, refractory wall surface and gas zone temperatures during operation. These models calculate gas zone temperature iteratively over a discrete number of time steps. The updated gas zone temperatures after each time step are used to calculate the heat flux to the stock and refractory wall surfaces. These heat fluxes are then used to calculate the new stock and furnace wall temperatures after each time step using a finite difference conduction model to simulate temperature changes internally within the stock and refractory walls. The transient zone models should be capable of reasonably accurate predictions of the load, refractory surface and gas zone temperatures as well as the required fuel input to heat the load to the desired temperature.

4.2 - The Energy Balance Equation

In accordance with the zone method of radiation analysis, an energy balance was formulated for each zone taking into account radiation interchange between all zones, Q_{rad}, the enthalpy transport, Q_{enth}, source terms associated with the flow of combustion products and their heat release due to combustion, Q_{Gnet} and Q_a (Rhine & Tucker, 1991). Also a term for the heat loss through the water cooling skid structure, Q_{wc}, is included in the energy balance.

$$Q_{Gnet} + Q_a + Q_{enth} + Q_{rad} - Q_{conv} - Q_{wc} = 0$$

The aim is to calculate all gas temperatures (T_g) such that the above energy balance is maintained for each gas zone *i*. The terms are defined as follows:

$$Q_{Gnet} = CV_{net} * m_{fuel}$$

$$Q_a = m_{air} * H(T_a)$$

$$Q_{enth} = \sum(m_{in} * H(T_g)) - \sum(m_{out} * H(T_i))$$

$$Q_{rad} = \sum \overrightarrow{GG_\iota} \sigma {T_g}^4 + \sum \overrightarrow{SG_\iota} \sigma {T_s}^4 - 4 \sum akV_i \sigma {T_g}^4$$

$$Q_{conv} = \sum A_j * h_j * (T_i - T_j)$$

$$Q_{wc} = \sum U * (T_i - T_{amb})$$

Where CV_{net} is the net calorific value of the fuel, *m* is mass (kg), *Ta* is the preheated air temperature (K), σ is the Stefan-Boltzmann constant (5.6687 x 10^{-10} kW m^{-2} K^{-4}), A_j is the surface area in the gas zone, h_j and *U* are heat transfer coefficients (kW m^{-2}) and T_{amb} is the ambient temperature, *H*(*T*) is the enthalpy of the stoichiometric combustion products and the $\overrightarrow{GG_\iota}$, $\overrightarrow{SG_\iota}$ terms Directed Flux Areas (DFAs).

4.3 - Calculation of Directed Flux Areas

The Directed Flux Areas (DFAs) allow for the effects of surface emissivity and the non-grey behaviour of the radiant interchange within the furnace enclosure. They relate the zone temperature to the TEAs and are calculated based on the mixed grey gas weighting coefficients that represent a real gas (Hottel & Cohen 1958):

$$\overrightarrow{G_\iota S_J} = \sum_{n=1}^{N_g} a_{g,n}(T_{g,i})(\overline{G_\iota S_J})$$

$$\overrightarrow{S_J G_\iota} = \sum_{n=1}^{N_g} a_{s,n}(T_j)(\overline{S_J G_\iota})$$

$$\overrightarrow{S_\iota S_J} = \sum_{n=1}^{N_g} a_{s,n}(T_i)(\overline{S_\iota S_J})$$

$$\overrightarrow{G_\iota G_J} = \sum_{n=1}^{N_g} a_{g,n}(T_{g,i})(\overline{G_\iota G_J})$$

The four-term mixed grey gas model (1 clear and 3 grey gases) weighting coefficients $a_{g,n}$ for calculating the directed flux areas are expressed as a low order polynomial in both T_g and T_i using other correlation coefficients, *b* as follows:

$$a_{g,n}(T_{g,i}) = b_{1,n} + b_{2,n}T_{g,i} + b_{3,n}{T_{g,i}}^2$$
$$a_{s,n}(T_i) = b_{1,n} + b_{2,n}T_i + b_{3,n}{T_i}^2.$$

The *b* coefficients and gas absorption coefficients *k* for Mixed Enhanced Gas (MEG) are shown in table 4.1.

	b_1	b_2	b_3	k_g
1	0.245283	1.13E-04	3.07E-08	0.00
2	0.28441	0.000185	-8E-08	1.05
3	0.38003	-0.00022	3.33E-08	14.30
4	0.090277	-7.3E-05	1.62E-08	240.50

Table 4.1 - Mixed Enhanced Gas (MEG) Coefficients (taken from Tata Steel)

One of the advantages in representing a real gas by a mixed grey gas model is that the absorption coefficients, k_g remain constant as they are independent of temperature and thus the weighting factors, $a_{g,n}$ will be used to take into account for the temperature dependency of the gas emissivity and absorptivity.

These directed flux areas take into account for multiple reflections within the enclosure and the non-grey absorption and emission of the combustion products. They are a function of temperature of the radiating emitter and are calculated from sets of direct and total exchange areas which must be evaluated for all zone pairs within the enclosure where the gas can be represented by a mixture of grey gases. Therefore the directed flux areas describe the complete radiative energy exchange between zone pairs within a furnace enclosure containing intervening non-grey gases.

Figure 4.1 represents the radiant energy balance Q_{rad}, for both a surface and volume zone and it is essentially the difference between all the radiation arriving at that zone and all the radiation leaving that zone.

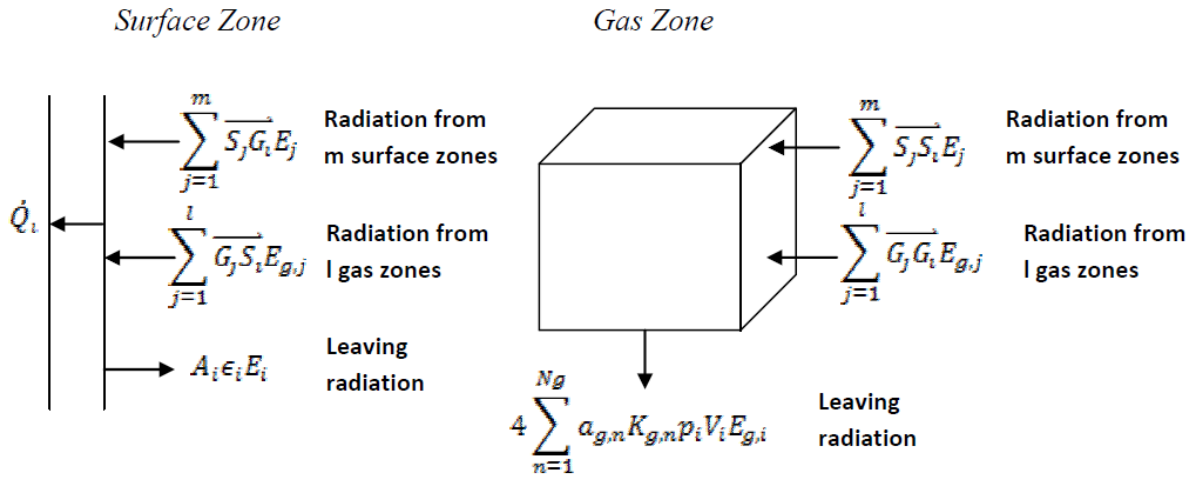

Figure 4.1 - The radiant energy balance at a surface and volume zone *i* (Correia S, 2001)

4.4 - Calculation of Enthalpy

When considering a simple long furnace such as that shown in figure 4.2, the enthalpy term of the energy balance equation Q_{enth}, is essentially the enthalpy arriving at zone *i* from all adjacent zones, minus the sensible enthalpy leaving zone *i* to all adjacent zones and the enthalpy loss due to the output flow of combustion products.

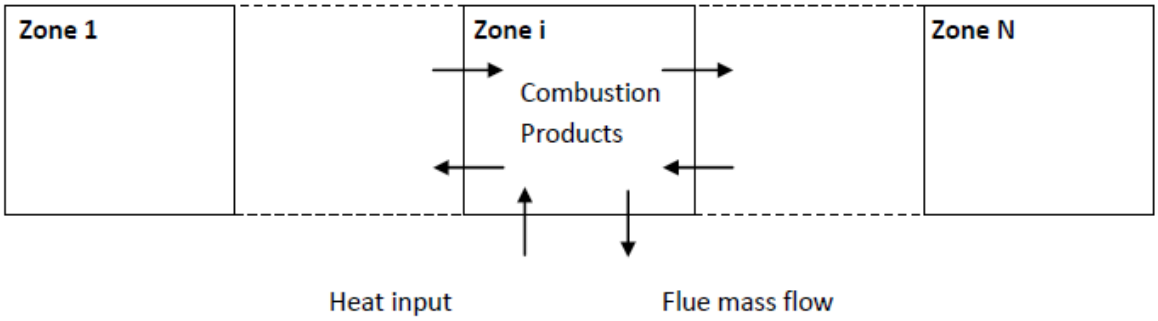

Figure 4.2 - Enthalpy flow representation for a long furnace model

The temperature-dependent specific enthalpy for the air and stoichiometric combustion products $H(T)$ was calculated by a volume-weighted average and fitted using the following polynomial correlation method:

$$H(T) = a + bz + cz^2 + dz^3 + ez^4 + fz^5$$

Where:

$$z = (T - 1400)/200$$

The coefficients that are to be used in the calculation to find the specific enthalpy of air are given in Table 4.2 and the coefficients to find the specific enthalpy of the MEG fuel are given in Table 4.3.

a	*b*	*c*	*d*	*e*	*f*
1.234164	0.243788	0.003322	-0.000059	0.000041	0.000006

Table 4.2 - Air polynomial coefficients (Rhine & Tucker, 1991)

a	*b*	*c*	*d*	*e*	*f*
1612.02	335.785	4.12034	-0.495308	0.0267341	-0.000494846

Table 4.3 - MEG fuel polynomial coefficients (Rhine & Tucker, 1991)

4.5 - Newton Raphson Method

The energy balance equations for each gas zone will give a set of *n* equations with *n* unknowns that can be solved using the Newton Raphson Method (Hildebrand, 1987) to obtain all T_g. Where X_k is the matrix of current temperature values for each gas zone *i* and $H^{-1}$is the inverse of the Jacobian matrix for the set of simultaneous equations, the following calculation is performed:

$$X_{k+1} = X_k - H^{-1}(X_k)F(X_k)$$

Rewording this for *E*, which is the difference between the next and current iteration gives:

$$E = X_k - X_{k+1} = H^{-1}(X_k)F(X_K)$$

Hence:

$$F(X_{k+1}) = F(X_k) - E$$

Each element of $H(X_k)$ where f_i is the energy balance equation for gas zone *i* and x_j is the temperature of gas zone *j*, is given as:

$$\delta f_i / \delta x_j = (f_i(x_j) - f_i(x_j + \Delta x_j)) / \Delta x_j .$$

The Newton Raphson iterations are repeated until the gas temperatures converge to within a given tolerance. Once the T_g values are calculated the heat flux (Q_i) to each surface zone can be calculated where ε_i is the surface emissivity of surface *i*.

$$Q_i = \sum \overrightarrow{GS_\iota} \sigma {T_g}^4 + \sum \overrightarrow{S_J S_\iota} \sigma {T_s}^4 - A_i \varepsilon_i \sigma {T_i}^4 + A_i h_i (T_g - T_i)$$

4.6 - 1D and 2D Conduction

The zone model includes a 1D (for refractory walls) and 2D (for stock) finite-difference transient conduction model to simulate the effects of conduction in the furnace walls and steel load. Even though the steel blooms are represented as 3D objects, 2D conduction as opposed to 3D conduction was used. This is due to the fact that the cross-sectional area of the 'ends' of the blooms was relatively small compared to the blooms length, meaning that these surfaces would receive only a small amount of radiation compared to the other sides of the bloom. This extra dimension of conduction would have a negligible effect, and the complexity of including this would give little benefit to the accuracy of the model.

The conductive heat transfer can be solved by the finite difference technique where internal temperatures are updated over a discrete number of time steps, from the initial conditions. It is, however, more accurate and stable (especially when a larger time step is needed to reduce the number of steps involved in the calculation) to use the implicit scheme, where, the arithmetic mean of the temperatures at the beginning and the end of each time step is used to determine the conduction into and out of each node. This approach, known as the Crank-Nicolson method (Crank & Nicolson, 1947), lead to a set of simultaneous equations which must be solved at every time step. However, the Crank-Nicolson method can be

computationally intensive so an appropriate step length must be used. For this study a fully explicit method was used with a suitable time step, found by trial and error that reduces computing time whilst ensuring stability. It is assumed that a constant heat flux, calculated by the zone model (which includes convection) is applied to the internal walls, roof and hearth of the at each time step. The finite difference conduction models use 10 equally spaced nodes in the dense refractory walls.

The 2D conduction model requires the heat flux to the side of the individual blooms to be known. An example of a 2D node arrangement is shown in figure 4.3.

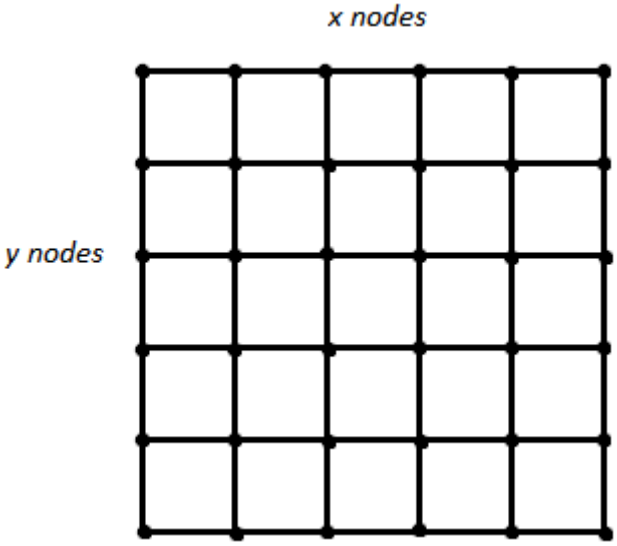

Figure 4.3 - Conduction Nodes

It is important at the end of each time step to account for the movement of the load. The load is moved throughout the furnace and discharged according to the furnace throughput rate. The transport of the blooms along the furnace from the charge end to the discharge end was simulated by simply shifting forward the bloom temperature at each walk interval of 'X' seconds (which will vary depending on the furnace throughput rate). In doing so, the temperature of the first bloom at the charge end is initialised to ambient conditions, therefore simulating charging of cold blooms. This process is achieved by the use of arrays within the model. These arrays keep track of time, bloom temperature after each time step and bloom position within the furnace chamber (the furnace can hold a max of 100 blooms). The conduction model uses the same polynomial method to calculate specific enthalpy is used to determine the specific heat and thermal conductivity.

$$Cp(T) = a + bz + cz^2 + dz^3 + ez^4 + fz^5$$

$$\lambda(T) = a + bz + cz^2 + dz^3 + ez^4 + fz^5$$

Table 4.4 shows the coefficients needed to calculate the specific heat for the refractory walls while table 4.5 lists the coefficients to calculate the specific heat of the stock at various temperature intervals, this is due to the discontinuities in these properties which occur between 723 and 800°C.

a	*b*	*c*
1001.64	0.1583	-4.58133E-05

Table 4.4 - Refractory Specific Heat Coefficients (Rhine & Tucker, 1991)

	A	*b*	*c*	*d*	*e*
0-750 °C	459.389	0.927605	-0.00893	0.000042717	-8.23237E-08
750 - 900 °C	9604.97	31.1055	-0.08219	-9.96642E-06	-2.91067E-09
> 900 °C	595.783	0.80929	-0.00172	1.13957E-06	-9.46037E-11
	F	*g*			
0-750 °C	6.17737E-11	-8.85174E-15			
750 - 900 °C	1.66675E-10	-1.12167E-13			
> 900 °C	-7.62604E-14	-			

Table 4.5 - Mild Steel Specific Heat Coefficients (Rhine & Tucker, 1991)

Table 4.6 shows the coefficients needed to calculate the conductivity for the refractory walls and table 4.7 gives the coefficients to calculate the conductivity of the stock below and above 800 °C.

A	*b*	*c*	*d*
1.8406105	0.000101183	-5.16367E-08	1.27786E-10

Table 4.6 - Refractory Conductivity Coefficients (Rhine & Tucker, 1991)

	A	*b*	*c*	*d*	*e*
0-800 °C	51.9059	-0.000369417	-7.68098E-05	-8.1131E-09	2.12134E-10
> 800 °C	30.2492	-0.0155686	1.44759E-05	-9.82726E-09	1.59948E-11
	F	*g*			
0-800 °C	-1.80744E-13	-			
> 800 °C	-9.36461E-15	1.48732E-18			

Table 4.7 - Mild Steel Conductivity Coefficients (Rhine & Tucker, 1991)

The surface temperatures are then updated and fed back to the energy balance program. The continuous transport of the blooms was simulated by a series of discrete pushes at fixed time intervals. At each push, one bloom was discharged, and the positions of all remaining blooms (together with their nodal temperatures) within the furnace were shifted forward towards the discharge end. The first bloom position at the charge end was then substituted with a new bloom at ambient temperature. This is repeated for many iterations until the gas and surface temperatures converge within a specified tolerance.

The output of the program will be the final gas, wall and stock temperatures. Figure 4.4 shows the flow chart for the energy balance program.

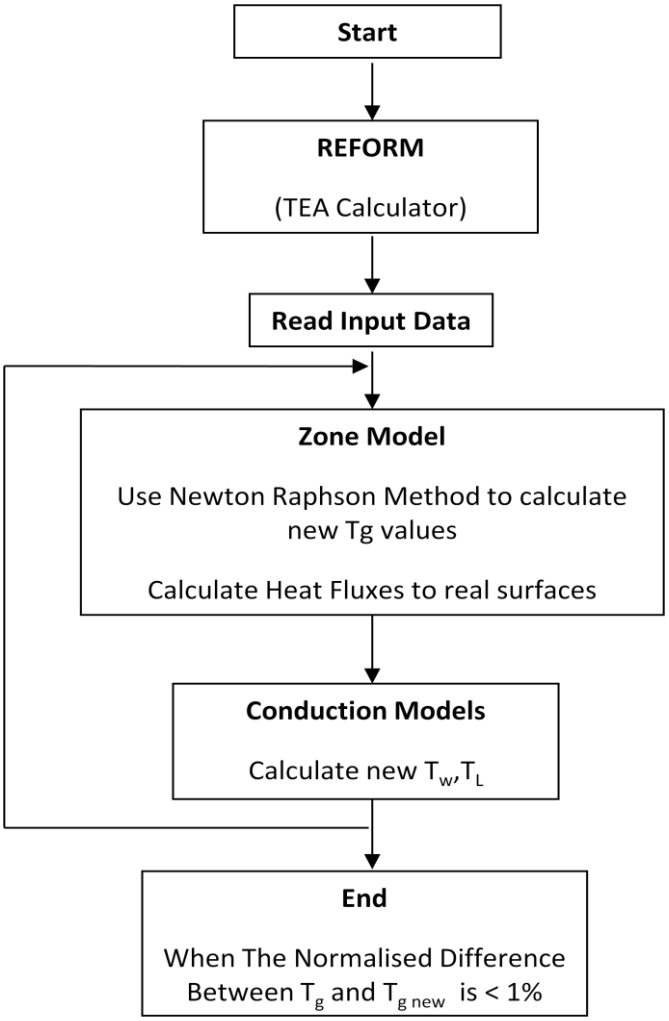

Figure 4.4 - Flow chart of Energy Balance Calculator

4.7 - Summary

Now that the method behind both the transient zone model and the radiation calculating program REFORM has been explained, the next chapter will investigate the results of both, comparing against existing data and analytical solutions.

Chapter 5 Results of the 3D Transient Zone Model

5.1 - The Reheating Furnace

The furnace that is being investigated for this research project is a top and bottom fired walking-beam furnace, located at Tata Steel's Scunthorpe Rod Mill (SRM). The schematics of the SRM (figure 5.1) show that it is 44.8m long, 10.2m wide and has a maximum height of 4.6m with an inclined roof which slopes down to 3.8m. The function of the furnace is to heat steel blooms to a desired drop-out temperature of around 1200°C, using a mixture of combustible fuel gases arising from the steelmaking process where the excess air level is maintained constant at 5.5%. Exhaust gases are removed from the furnace via two flues at the charge end which are then used to preheat the incoming combustion air by means of a recuperator which operates with an efficiency of 50%. The furnace has a total of 75 burners, where 51 of are nozzle mix and they are arranged to fire above and below the blooms. The furnace can hold a total of 100 blooms and it operates continuously such that as a cold bloom enters the charge end a hot bloom is discharged at the opposite end. The throughput rates of the furnace can vary giving a total thermal input to the burners of up to 60MW.

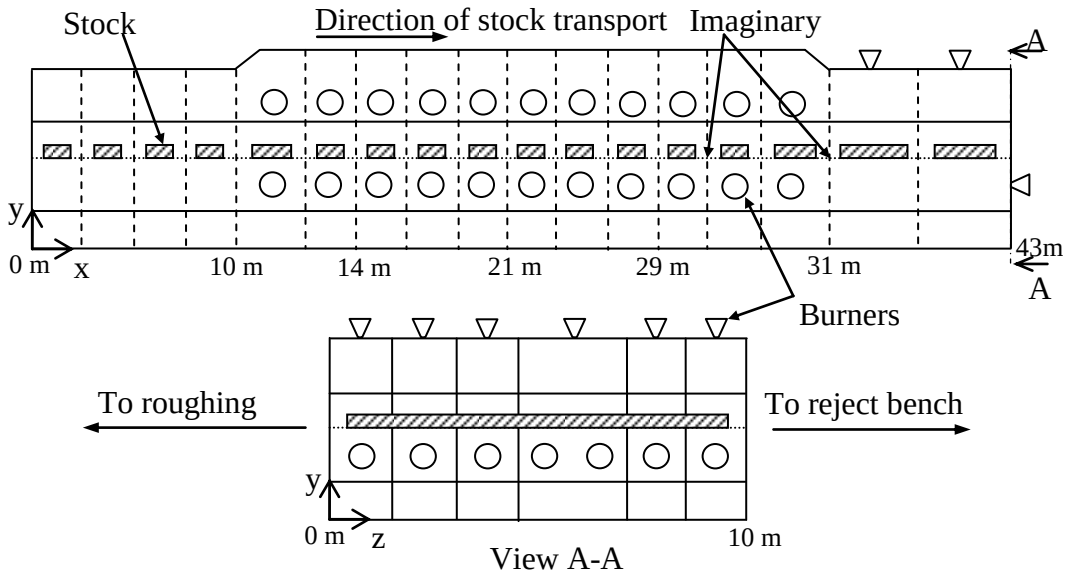

Figure 5.1 - Schematic Representation of the TATA Steel SRM Furnace (taken from TATA Steel)

The process of the mill is split into several different, from the start of the process where a cold bloom enters the re-heating furnace to the end of the process where the coils are

formed and inspected. The billet and bloom reheating furnace reheats billets and blooms to a discharge temperature of around 1150°C to 1200°C in preparation for the rolling process. It has a maximum throughput of 200 tonnes and uses mixed enhance gas which is generated on the Scunthorpe site.

5.2 - REFORM Validation

5.2.1 - Summary of the Method

All tests were performed using implementations in the C# 2010 programming language, running on a 2.93GHz quad core Intel i7 CPU computer. Testing REFORM on the full TATA SRM furnace, with 2,000 Rays per square metre and 100 obstacles, the time taken to calculate all view factors with exhaustive checking is 923 seconds. The addition of voxel traversal when employing the bounding volume approach reduces this to 340 seconds. As the bundle of rays leaving a particular zone is independent of bundles leaving other zones, the calculations can be run in parallel, thereby further decreasing processing time (Howell, 1997). The more processors are available, the more bundles can be investigated simultaneously. Parallel processing reduces running time yet further to 136 seconds. The larger the furnace (increasing numbers of surface and volume zones), the larger is the proportionate reduction in processing time owing to the use of voxel traversal.

5.2.2 - REFORM Results and Discussions

This section describes the validation of REFORM. Comparison is first made between REFORM and analytically calculated values. View factors derived analytically for pairs of zones in the SRM furnace are compared to those calculated by REFORM with increasing numbers of rays to determine a ray density that will give an absolute percentage difference of less than 5%. REFORM is then compared to RADEX by consideration of TEAs. REFORM and RADEX were used to model the SRM furnace without obstacles present, as the latter cannot afford representation of obstacles sufficiently well to enable comparison. Finally REFORM is used to simulate the SRM furnace with varying numbers of obstacles to determine whether the program predicts realistic trends in view factors.

5.2.3 - Ray Density Investigation

The following logarithmic chart (figure 5.2) compares the view factors between two zone pairs calculated by an analytical method (Incropera & De Witt, 1990) with the averaged view factors calculated by several runs of the new MCRT method using a variety of ray densities to investigate the effect of density on accuracy.

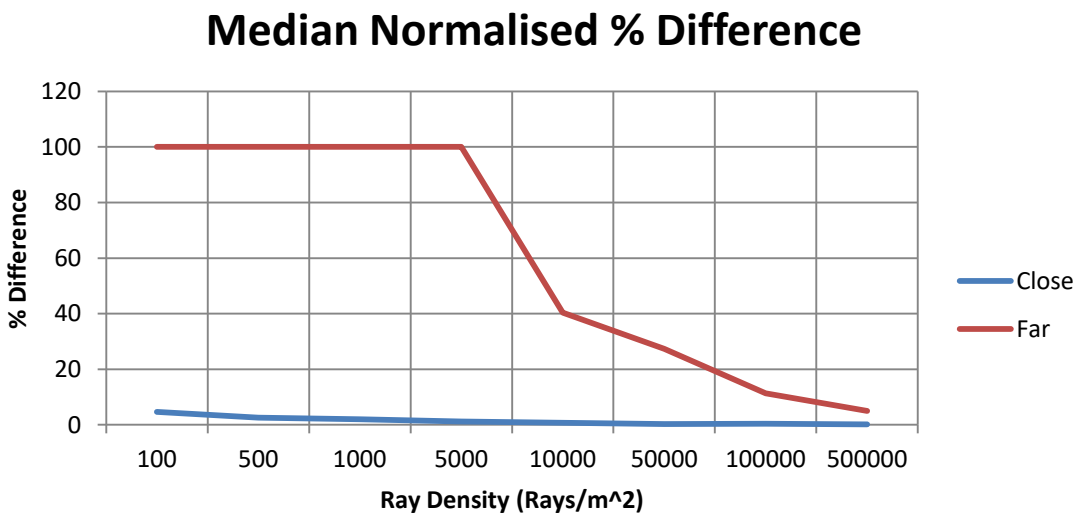

Figure 5.2 - Average Error Percentage Compared to Analytical Values

As REFORM uses the Monte Carlo method, increasing the number of rays increases the statistical accuracy. The percentage error between the analytical values and REFORM using 5000 rays per square metre means that DEA calculations on a furnace of this size gives values that are accurate to within ±5% (±1% for close pairs). For larger furnaces a greater ray density will need to be used to reach this accuracy as the view factor between distant zone pairs is very susceptible to statistical error when using the Monte-Carlo method.

5.2.4 - Comparison with RADEX

The following table (5.1) shows the median, mean and maximum percentage differences in the calculated TEAs between REFORM and RADEX from a particular sending surface zone to the closest 70 surface zones out of the 120 defined (which takes into account over 99% of the zones' DEA contribution).

Number of Rays	Median Difference %	Mean Difference %	Max Difference %
200000	5.62	6.43	21.6
400000	3.98	4.17	16.8
600000	2.22	2.47	12.5

Table 5.1 - REFORM compared with RADEX

Table 5.1 shows that the agreement between the programs improves as the number of rays is increased, and the differences between them is sufficiently small to regard their outputs as comparable. The reason for this difference is that the Monte Carlo method is a statistical method and surface zone pairs that are further apart are more susceptible to random difference. The closeness of the mean and median difference values shows the influence of more distant TEAs, which act as outliers due to their higher statistical variability. As the contribution to radiation exchange from these distant zones (other than the closest 70 zones) constitutes less than 1% (in terms of their TEA), the differences in calculated TEAs will be insignificant.)

5.2.5 - Simulation of Full-Scale furnace

Now that agreement between REFORM, RADEX, and analytical values has been established, REFORM is used to model a full-scale rod mill (SRM) furnace with obstacles represented individually and the radiation interchange calculated between top and bottom parts of the furnace; which are separated by the intervening stock (figure 5.3a). The TEAs between all top and bottom zone pairs are calculated to show trends when the number of obstacles on the walking beam is varied. All obstacles are of equal size, with equal spacing between obstacles, in each run. The horizontal axis of the contour plots shown in figure 5.3b-d indicates the particular zone of the bottom zones, where zero represents the first zone from the origin; similarly the vertical axis represents the top zones. Points on the graphs that have the same horizontal and vertical coordinate (which make up the main diagonal) are therefore directly opposite each other. If the bottom zone number does not match the top this means the zones are offset from each other; the greater the difference between zone numbers, the greater the magnitude of this offset. The greyscale chart represents the

magnitude of the TEAs, where the greater the TEA value the brighter the point is on the contour plot.

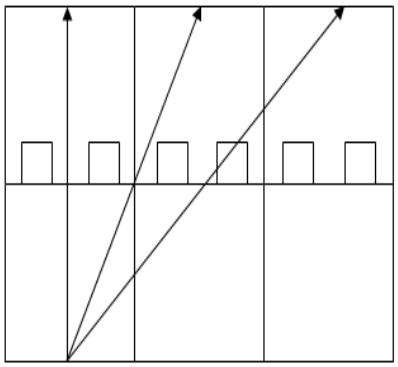

(a)

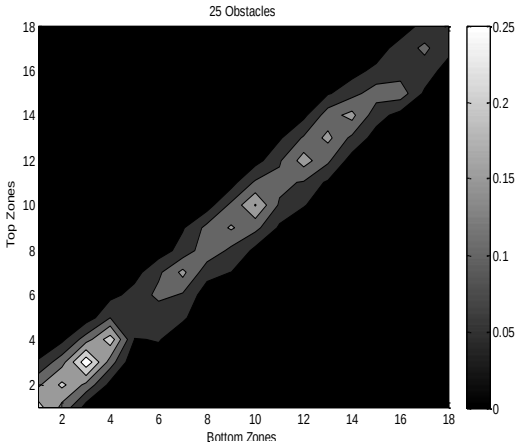

(b)

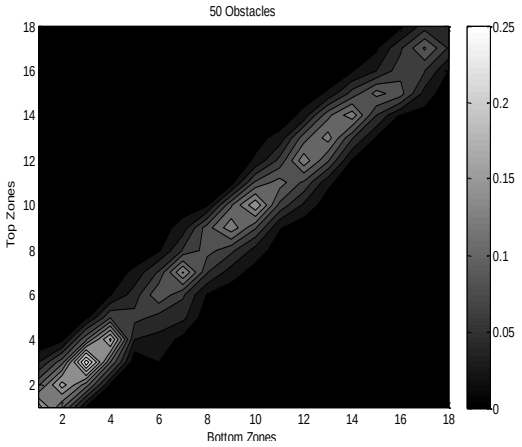

(c)

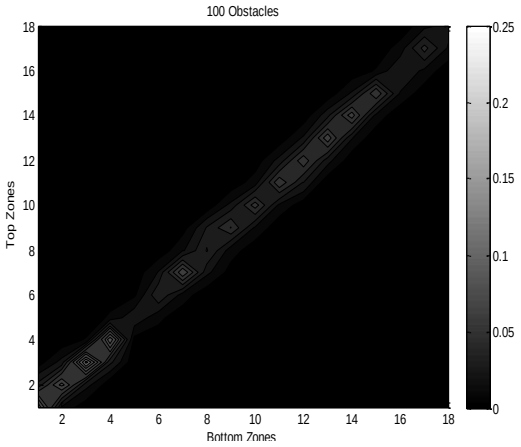

(d)

Figure 5.3 - SRM Total Exchange Area Contour Plots with Decreasing Spacing Between Obstacles: (a) Illustration of Ray Interactions with Objects; (b) 25 Obstacles, (c) 50 Obstacles, (d) 100 Obstacles.

The contour plots shown in figures 5.3b-d show that the TEA is greatest between zones that are directly opposite each other as this is the shortest distance. The general trend observed is that zone pairs that are further away have a smaller TEA than those close together, which is consistent with the fundamentals. Moreover, decreasing the gap between obstacles decreases the TEA due to the view between top and bottom pairs being more obstructed by the increase in number of obstacles. It is also clear that as the gap between obstacles increases the directionality of the radiation interchange becomes more significant as indicated by the contour brightness across the width of diagonal. These results show that REFORM is capable of simulating the influences of obstacle dimension and spacing on radiation interchange between the top and bottom section of the furnace. As there are no large areas of zero TEA along the main diagonal of the contours for the 100 obstacle test this proves that the program represents all the obstacles in a particular volume zone individually with gaps in between them. The summation rule is also satisfied which means that each ray only hits exactly one surface zone which is an important factor for validation.

5.3 – 3D Transient Model Results

The first set of results was obtained for a 3D furnace model. The enthalpy flows were taken from a CFD simulation snapshot of the flows calculated by researchers at the University (Jenkins *et al* 2011a, 2011b) and scaling them uniformly by a factor such that the stock would reach the desired discharge temperature.

It is assumed that all gas zones in the model are assumed well stirred, i.e. they have uniform composition and temperature. The surrounding surface zones are also assumed to be isothermal as well as grey and diffuse. The emissivity of the furnace walls is a function of temperature, but for simplicity REFORM assumes that emissivity is constant, which is typical of the refractory material used at average furnace operating temperature (Correia, 2001). The emissivity of the load increases from 0.6 to 0.8 in a linear profile the further the stock is into the furnace. The thermal conductivity and specific heat capacity of the refractory surfaces was also assumed to be constant (Rhine & Tucker, 1991). However, the thermal conductivity and specific heat capacity of the stock (mild steel) are taken from data collated by (Rose & Cooper, 1977).

The calorific value and chemical composition of the fuel are those calculated for the mixed enhanced gas. Combustion of the fuel was assumed to be fully completed within the volume

zones adjacent to the burners. The convective heat transfer between the gas zones and their adjacent surface zones was also taken into account. Previous mathematical models of furnaces have either ignored convection or used an empirical value to represent the heat transfer coefficient (Anton J. T., 2005). An estimation of convection was used in this study for zone modelling purposes. The heat loss to the water-cooled transport skids from each volume-zone was assumed to be proportional to the exposed surface area of skids in that zone. For simplicity, rather than modelling the geometrical effects of shadowing of the entire walking-beam structure, a uniform reduction on the incident radiant heat flux on the bottom load surfaces can be assumed (Zongyu *et al*, 1987). For transient simulation from cold start-up, it was assumed that the furnace refractory and load structures were initially at room temperature.

The zoning arrangement was based on the position of the nozzle mix burners (in the x-direction) to be able to fully represent the longitudinal temperature variations as shown in figure 5.4.

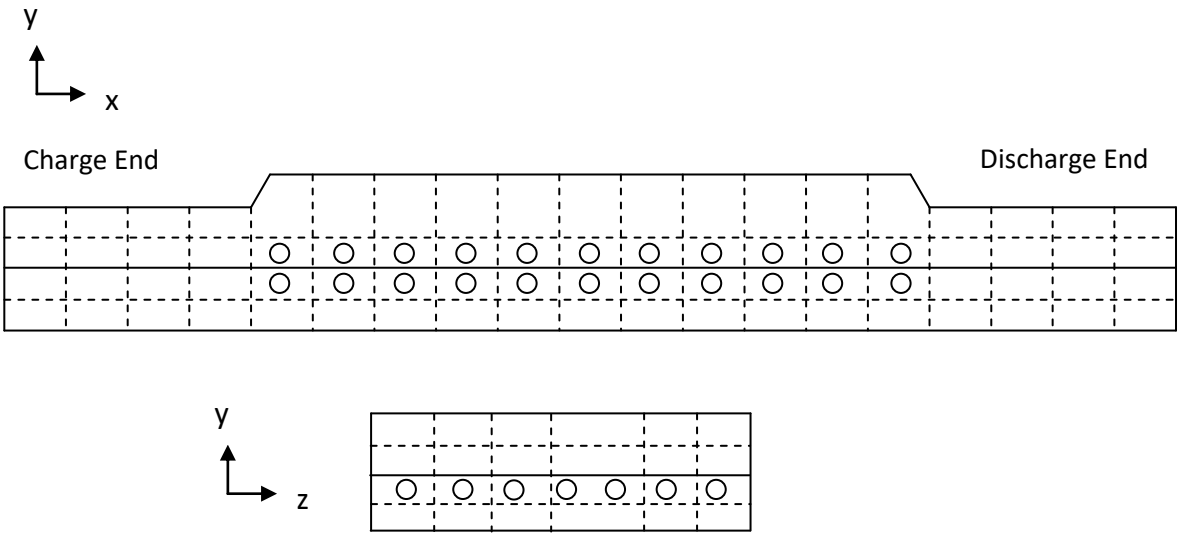

Figure 5.4 - Furnace Zone Arrangement

The enthalpy term Q_{enth} is calculated from the mass flow rates of the combustion gases between zones with the specific enthalpies evaluated at the temperature of the sending zone. The effects of temperature and combustion on the furnace flow patterns can often be excluded and therefore the isothermal flow patterns and radiation exchange areas can be

calculated outside of the zone model. The mass flow rates were determined by isothermal (at ambient temperature) Computational Fluid Dynamics (CFD) calculations carried out using Ansys Fluent. This only needs to be determined once for a given burner arrangement and firing condition as the magnitude of these flows relative to the burner flows will essentially be unchanged since the flows are turbulent.

A summary of the boundary conditions imposed are as follows:

- 3D Furnace Model: 19 *x* Gas Zones, 4 *y* Gas Zones and 6 *z* Gas Zones.
- Furnace Length: 44m
- Furnace Height: 3.8 - 4.55m
- Furnace Width: 10.2m
- Number of Blooms: 100.
- Bloom Length: 0.283m
- Bloom Height: 0.23m
- Bloom Width: 8.4m
- Initial Wall Temperatures: 20°C.
- Initial Gas Temperatures: 20°C.
- Initial Stock Temperature: 20°C.
- Fuel: Four Term MEG (1 Clear, 3 Grey).
- Enthalpy flows: Uniformly scaled CFD snapshot.
- Wall Emissivity: 0.9.
- Stock Emissivity linear profile: 0.6 - 0.8.
- Wall Material: Dense Refractory Brick.
- Heat Transfer Coefficient: 0.01 kW / (m^2K).
- Net Calorific Value: 11.72 * 10^3 kj / kg.
- Excess Air: 5.5%.
- Preheated Air Temperature: ~ 340°C.
- Node Spacing: 10 Nodes 1D Conduction, 5 * 5 Nodes 2D Conduction.
- Shadowing of bottom stock surface: 20%
- Delay: 5 Minutes after 90 Minutes.

Figure 5.5 shows the various predicted node temperatures of the stock at different positions within the reheating furnace.

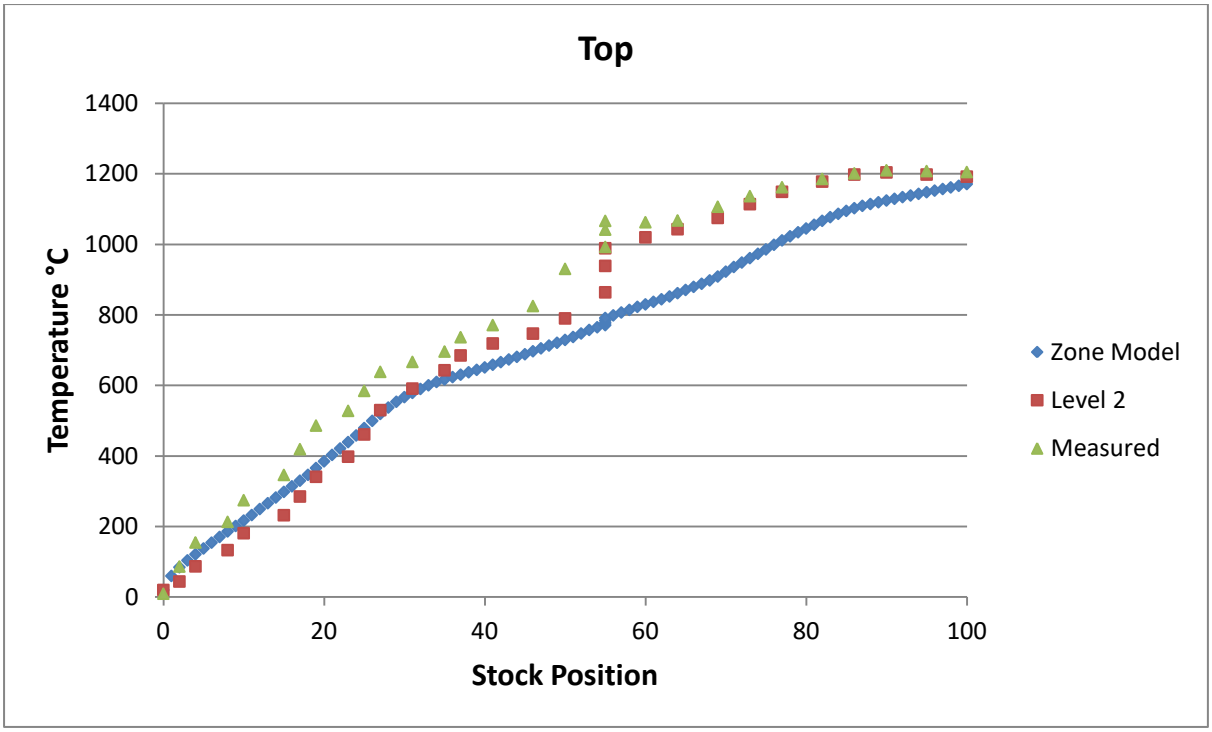
Top
Temperature °C
1400
1200
1000
800
600
400
200
0
0
20
40
60
80
100
Stock Position
Zone Model
Level 2
Measured

(a)

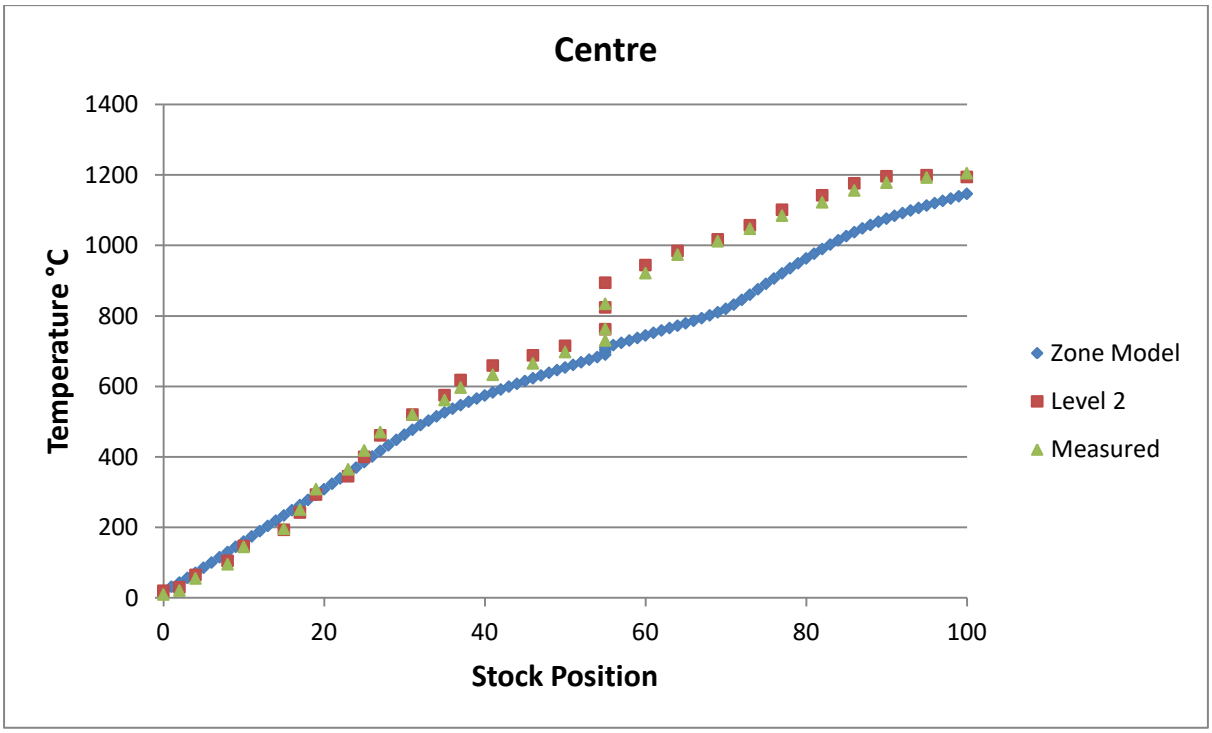
Centre
Temperature °C
1400
1200
1000
800
600
400
200
0
0
20
40
60
80
100
Stock Position
Zone Model
Level 2
Measured

(b)

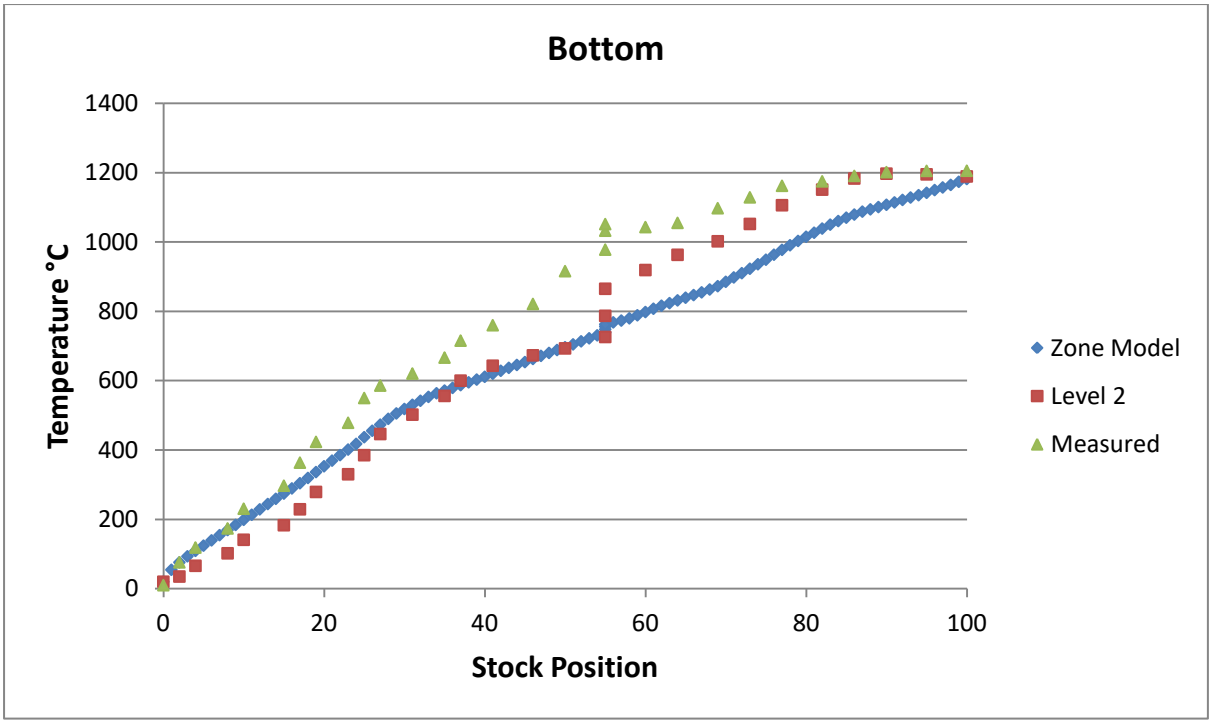

(c)

Figure 5.5 - 3D Model: 5 Minute Delay 20% Shadowing - Temperature of (a) Top (b) Centre (c) Bottom Stock Nodes

From figure 5.5 it can be seen that while the predicted stock node temperatures match those of the experiment data before the delay, the simulation under predicts the increase in temperature during the delay and after. The 3D model was found to take a very large amount of time to converge due to the number of gas zones. Also, while the discharge temperature was reached the profile did not match that of the experiment data. This is because uniformly scaling the enthalpy flows of a snapshot does not allow for a realistic representative of transient furnace operation.

5.4 - Summary

As the 3D model requires a large computational time a smaller model with less zones will be investigated in the next chapter. In addition to this, as the mass flows are unknown for a different zone arrangement, a plug-flow assumption will be used. This will allow for a temperature controller to be developed to regulate the fuel input in proportion to how the furnace is performing against set-point temperatures, instead of uniformly scaling a snapshot of mass flow rates from a CFD simulation.

Chapter 6 Transient Long Furnace Zone Model Development and Results

A LFM was developed, that has a reduced computation time compared to the 3D model and can be more efficiently used to investigate the affect of introducing a temperature controller. Also investigated in this chapter was the affect modelling the pulse fired nature of the burners to see whether this has an effect on the temperature profile and temperature uniformity within the stock. An LFM was chosen as this is ideal for using a plug-flow assumption and bypass running CFD simulations to calculate mass flow rates for different pulse firing patterns. This assumption will remove the limitations of previous models (Jenkins *et al* 2011a, 2011b) that relied on scaling of CFD snapshot mass flow rates.

In the LFMs there is essentially no temperature variation across the width and height in each furnace section so that only longitudinal variations were taken into account.

6.1 – LFM and Temperature Controller

The LFM has the same dimensions as the 3D model, however there is only a single split in the *z*-axis, making it a 2D model, atypical of most LFMs which are usually 1D. The mass flow rates were calculated as a proportion of the maximum mass flow into each gas zone from the burners connected to that gas zone as well as the plug -flow inter-zone mass exchange. A temperature is used to calculate the proportion of the burners maximum fuel input rate needed for the stock to reach the required temperature in a particular control zone. The furnace control zone layout displayed in figure 6.1 and burner capacities were supplied by Tata Steel.

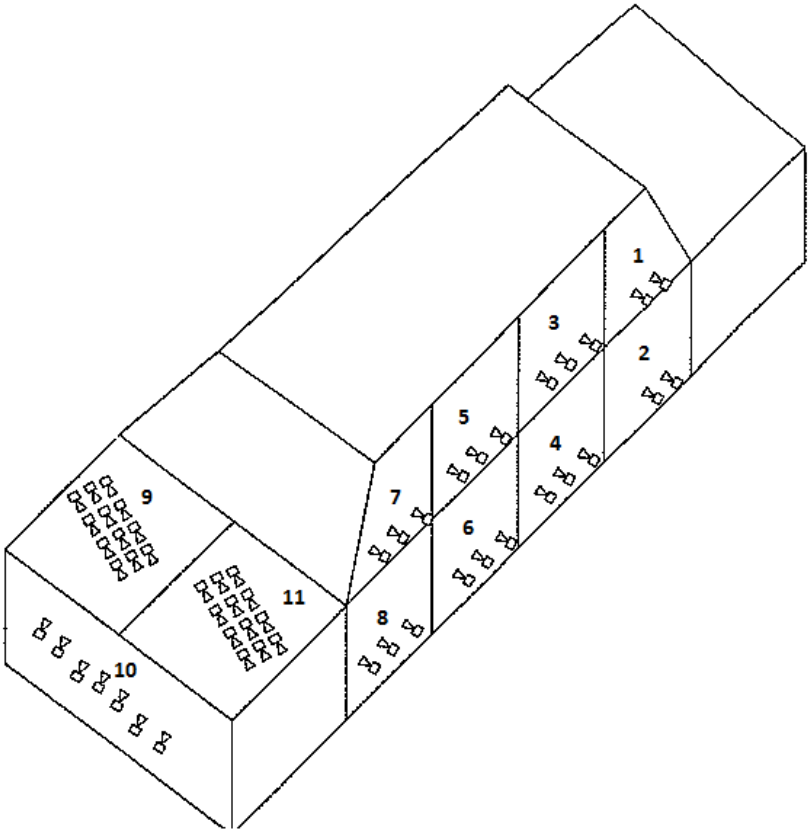

Figure 6.1 - SRM furnace control zone layout (taken from TATA Steel)

The temperature controller is designed as shown in figure 6.2 (Rhine & Tucker, 1991):

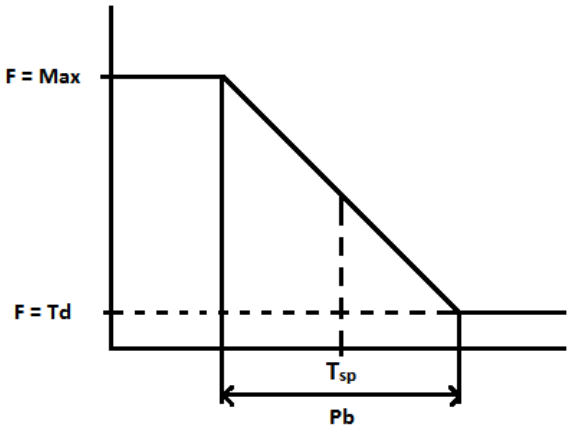

Figure 6.2 - Temperature Controller Function Graph (Rhine & Tucker, 1991)

Where *F* is the thermal capacity required, *Td* is the burners' lowest fuel capacity, T_{sp} is the set point temperature and *Pb* is the proportional band. If the actual temperature T_{act} is less than the lower limit of the proportional band the burners will be firing at maximum capacity. If the actual temperature is greater than the upper limit of the proportional band

the burners will be firing at minimum capacity. If the actual temperature is within the limits of the proportional band the following equation applies to determine thermal capacity required:

$$F = aT_{act} + b$$

Where:

$$a = (Td - 1)/Pb$$
$$b = \frac{Td+1}{2} - (Td - 1)(\frac{T_{sp}}{Pb}) .$$

6.2 – LFM 160 t/hr Results

The LFM that was implemented uses the same conditions as the previous simulation but with a plug flow assumption. It was also then possible to introduce the pulse firing technique and proportional temperature controller using particular set point temperatures. The new furnace zoning is then 17 *x* Gas Zones, 2 *y* Gas Zones and 2 *z* Gas Zones. The set point temperatures that are to be used in the temperature controller are shown in Table 6.1.

Control Zone	Set Point Temperature
1	900
2	900
3	901
4	901
5	1057
6	1066
7	1205
8	1205
9	1175
10	1175
11	1175

Table 6.1 - LFM - Initial Set Point Temperatures (taken from CFD Snapshot)

An investigation was conducted to determine the affect of varying ray density would have on the temperature profile of the stock.

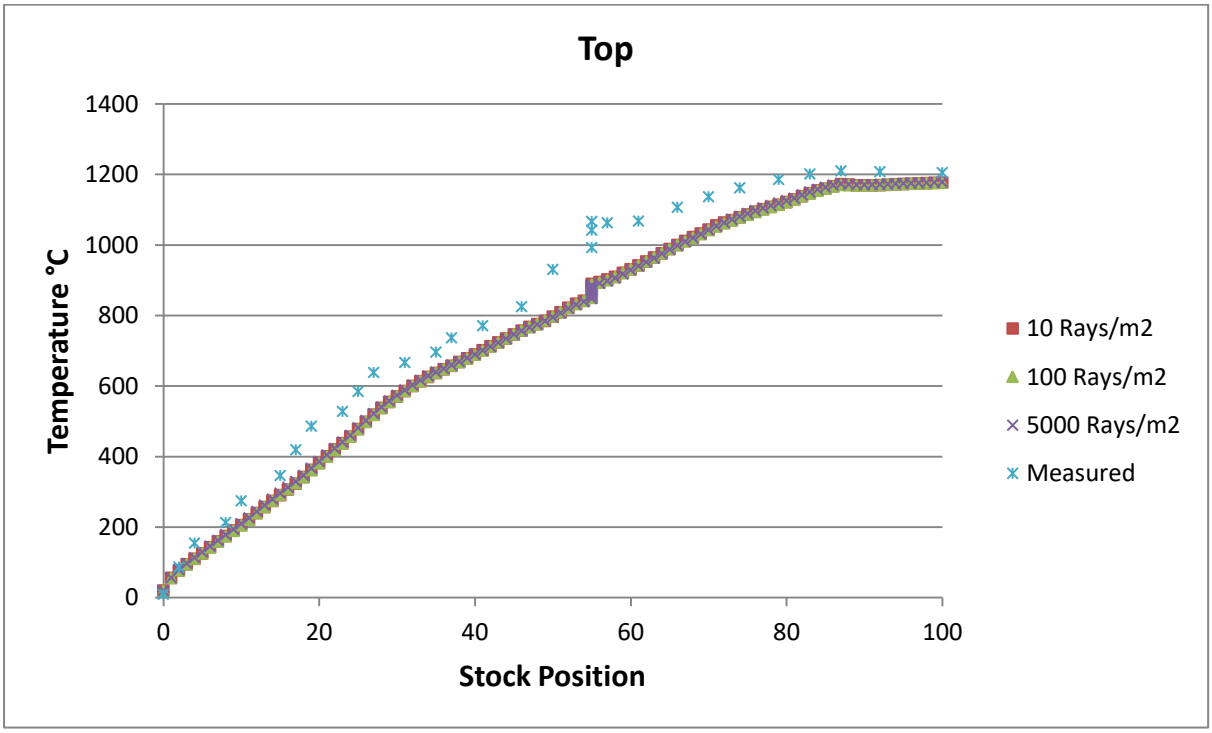

(a)

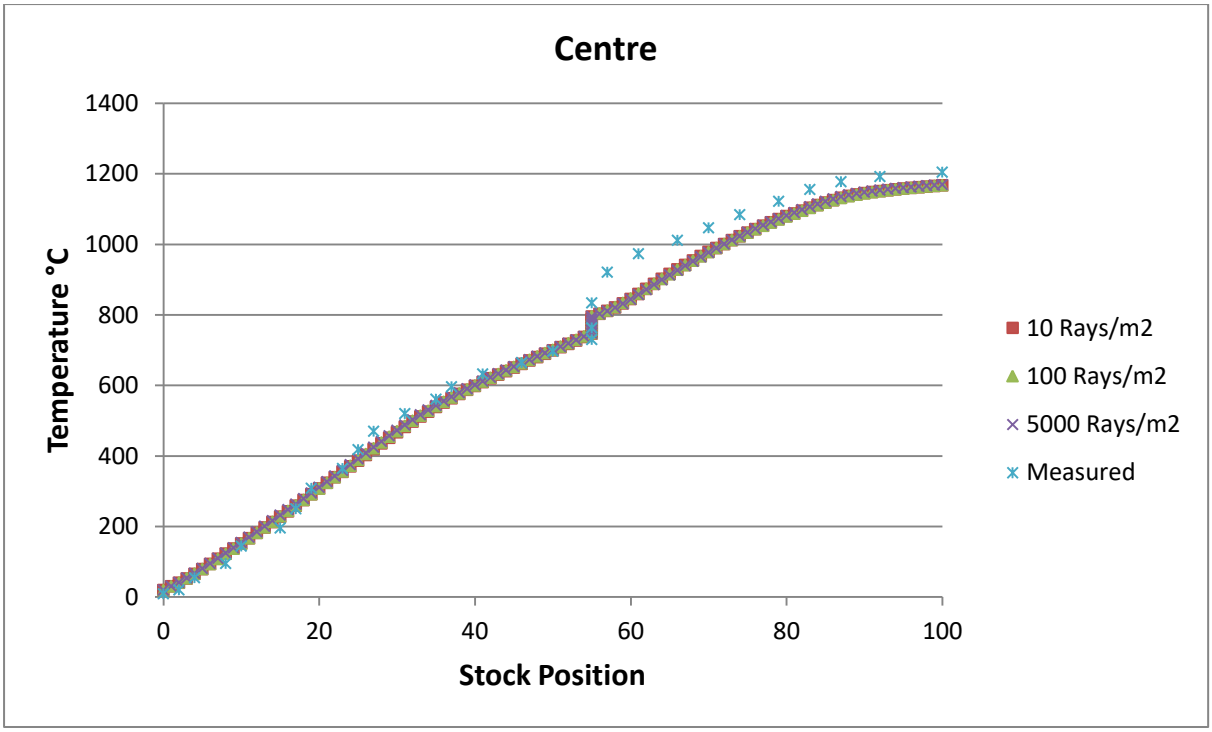

(b)

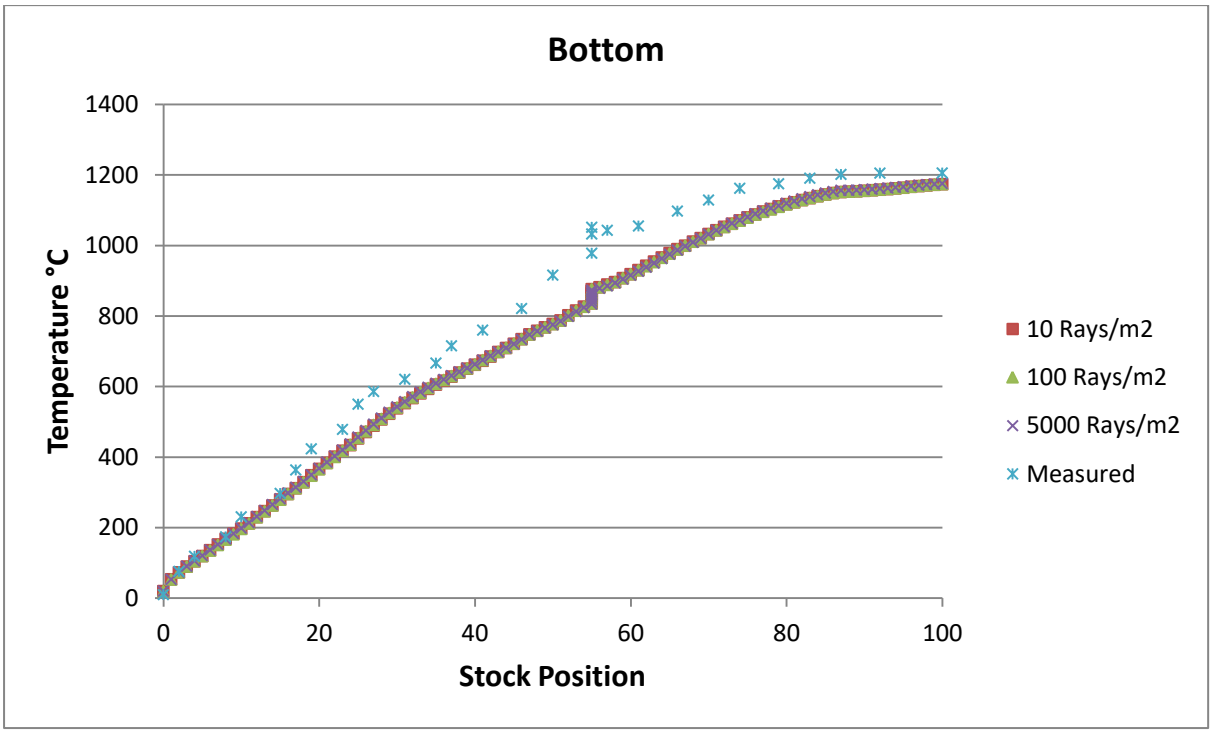

(c)

Figure 6.3 - LFM: Comparison of varying Ray Density - Temperature of (a) Top (b) Centre (c) Bottom Stock Nodes

It can be seen from figure 6.3 that varying the ray density greater than 10 rays/m^2 has a negligible effect of the stock temperature profile.

An investigation was also made to determine what level of shadowing should be applied to the bottom surfaces of the steel load to account for the obstruction of radiation to the stock by the walking beam. Various factors of shadowing were trialled and compared to the measured data to evaluate which compared best to the data.

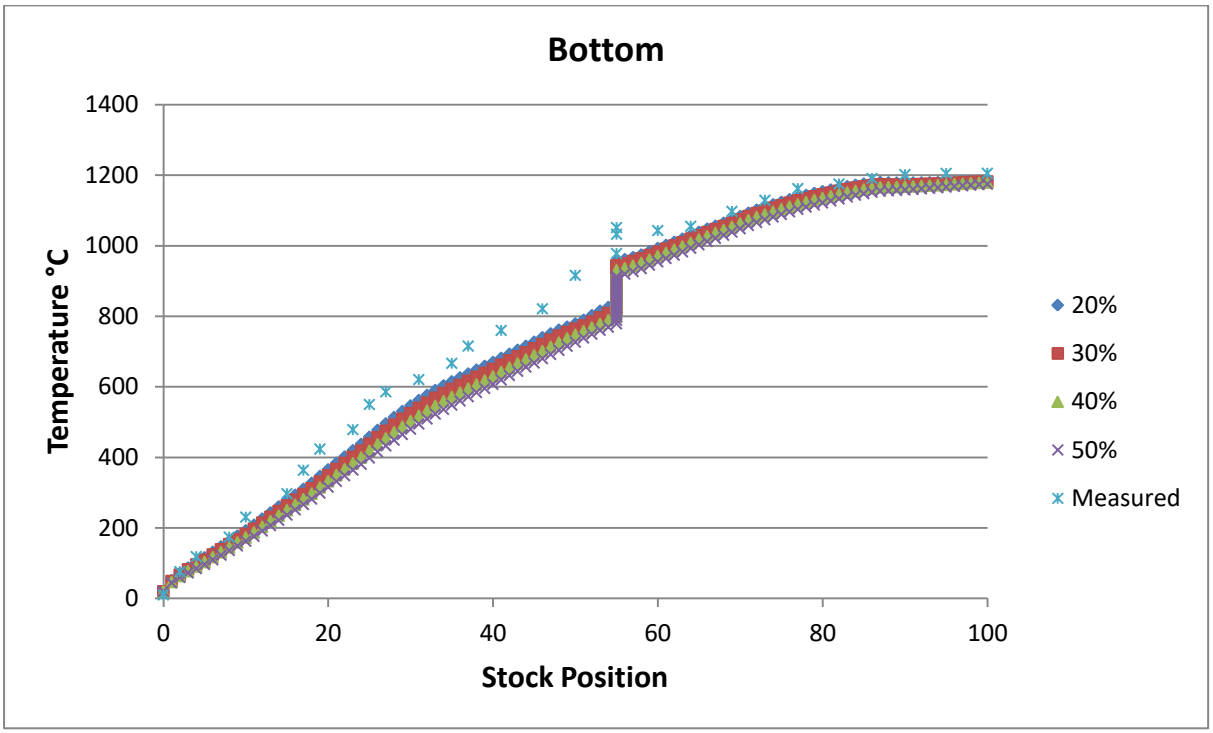

Figure 6.4 - LFM: Comparison of varying Shadowing % on Bottom Stock Nodes

Figure 6.4 shows that using 20% shadowing matches closest to the measured data so this will be used going forward.

The final investigation was to determine what length of production delay would give a similar uplift in temperature while the stock was stationary.

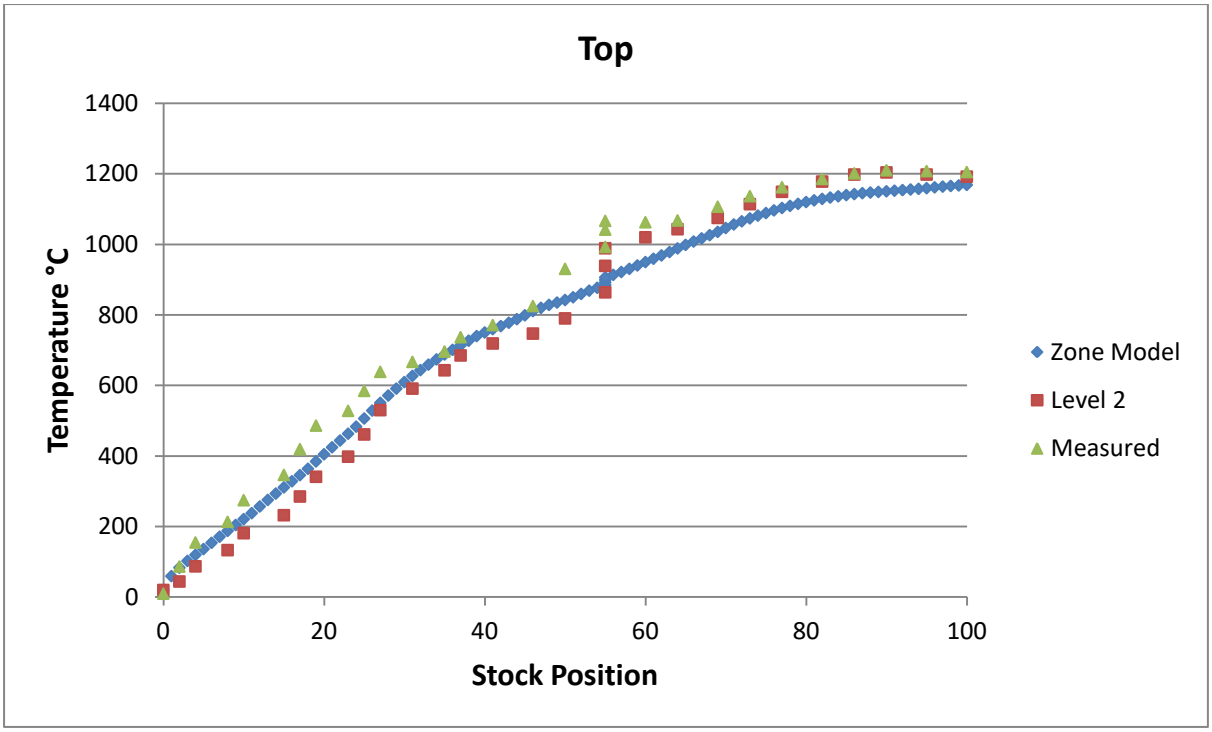
Top
Temperature °C
1400
1200
1000
800
600
400
200
0
0
20
40
60
80
100
Stock Position
Zone Model
Level 2
Measured

(a)

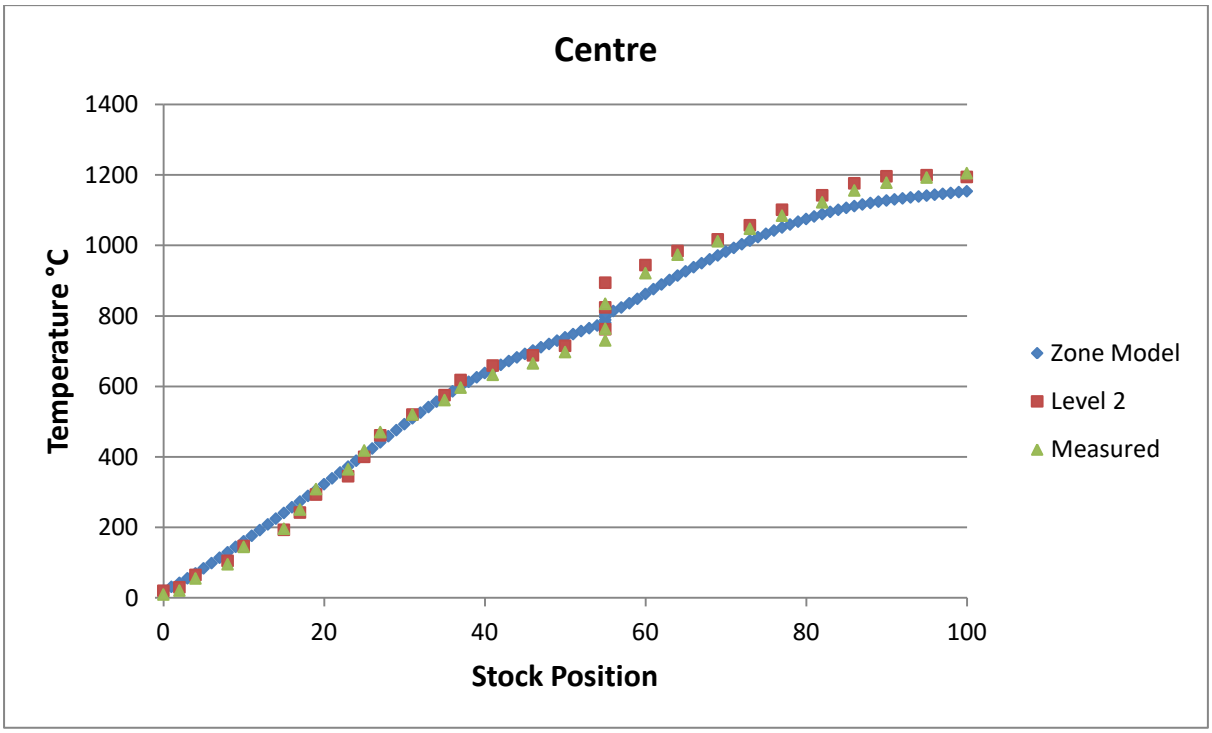
Centre
Temperature °C
1400
1200
1000
800
600
400
200
0
0
20
40
60
80
100
Stock Position
Zone Model
Level 2
Measured

(b)

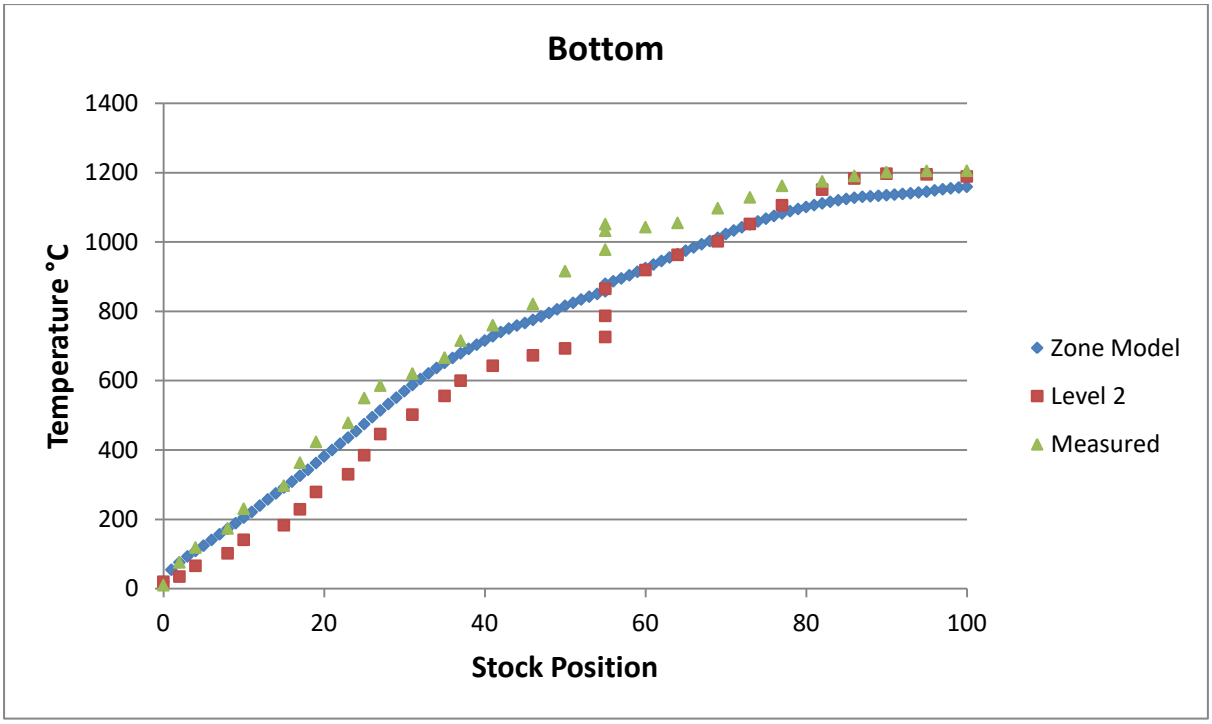

(c)

Figure 6.5 - LFM: 5 Minute Delay 20% Shadowing - Temperature of (a) Top (b) Centre (c) Bottom Stock Nodes

The results in figure 6.5 show that the simulated temperature increase during the delay was not as large as in the experiment data. To investigate this, increasing lengths of delays were simulated to better match the experiment data.

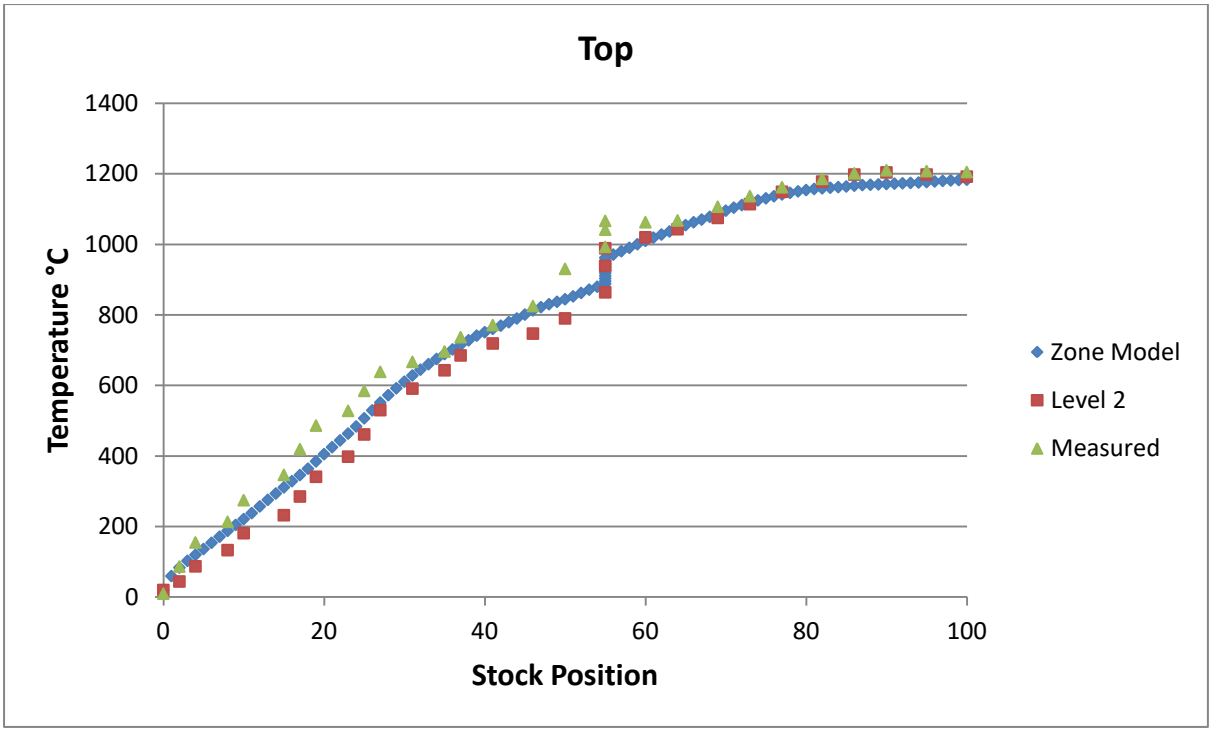
Top
Temperature °C
1400
1200
1000
800
600
400
200
0
0
20
40
60
80
100
Stock Position
Zone Model
Level 2
Measured

(a)

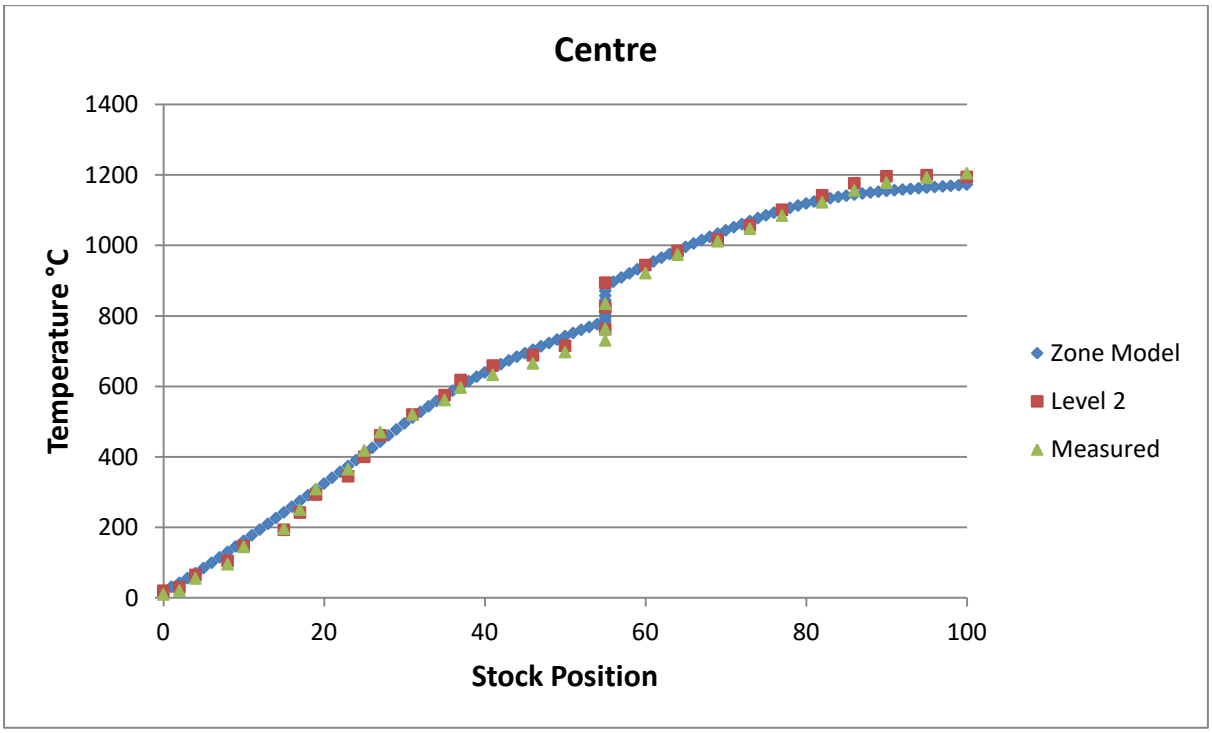
Centre
Temperature °C
1400
1200
1000
800
600
400
200
0
0
20
40
60
80
100
Stock Position
Zone Model
Level 2
Measured

(b)

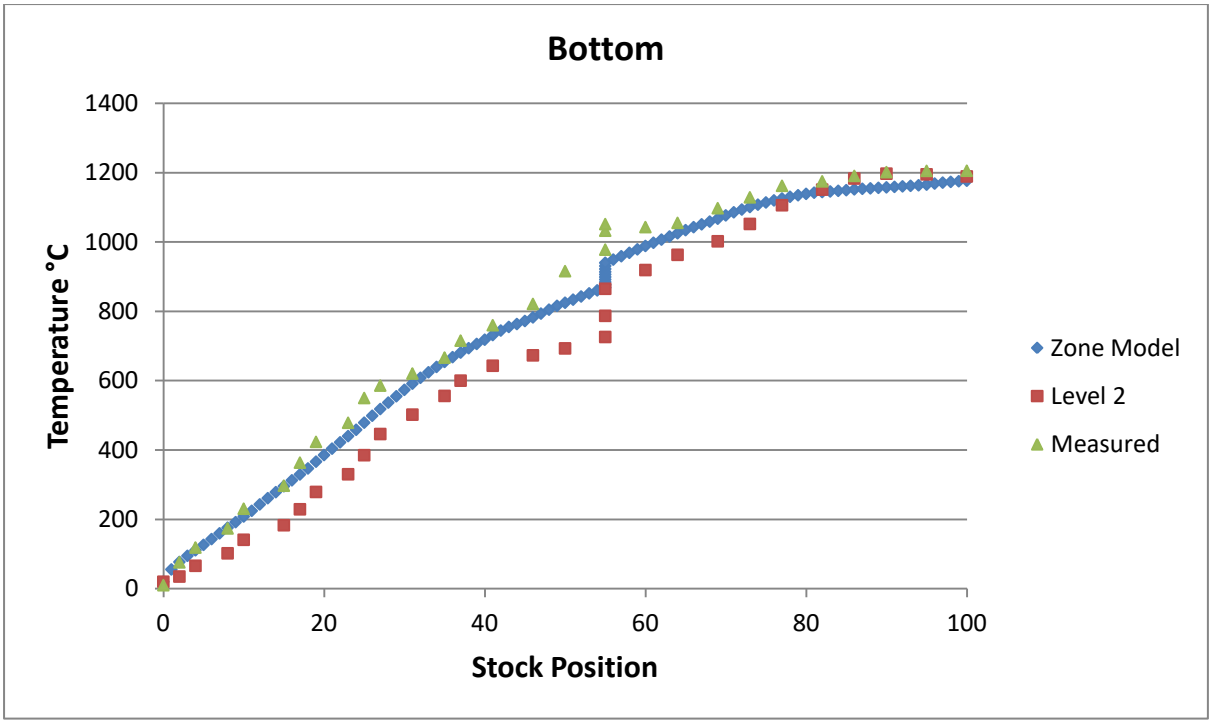

(c)

Figure 6.6 - LFM: 15 Minute Delay 20% Shadowing - Temperature of (a) Top (b) Centre (c) Bottom Stock Nodes

The temperature increase during the delay shown in figure 6.6 now closely resembles the trend of the experiment data.

	Energy In (MW)		
QG_{net}	79.3	**Preheat (°C)**	
Qa	10.0	340	
Total	89.3		
	Energy Out (MW)	**%**	**Tata %**
Qex	31.7	35.52	38.00
Qwc	15.6	17.45	19.00
Qwall	5.1	5.69	10.00
Qstock	36.9	41.34	45.00
Specific Fuel Consumption (GJ/Tonne)	1.78		
Maximum Stock Node Temperature Difference (K)	16.66		

Table 6.2 - Energy Balance Output for 160 t/hr Simulation

In table 6.2 the simulation energy balance outputs are compared to that of the similar SRSM furnace as no data is available for the SRM furnace. It can be seen that the energy distribution is reasonably similar to that of the SRSM furnace. The maximum stock node temperature difference, which is a measurement of temperature uniformity, is also acceptably close.

6.3 - Pulse Firing Technique

Once the thermal capacity has been calculated for each control zone, the correct pulse firing pattern needs to be calculated. If, for example, the thermal capacity is 50%, then half the burners should be firing for the pulse time, and after this pulse time has ended the burners that were firing should now be off and the burners that were off should now be firing. The following equations are used to determine the correct firing pattern:

$$W = ON/F$$

$$D_n = (W - ON) \times (n - 1)$$

Where N is the number of burners, ON is the burner pulse time, W is the pulse period and D_n is phase offset for the n^{th} burner.

The SRM furnace contains groups of four and six burners, the firing sequences assumed for each are shown in figure 6.7.

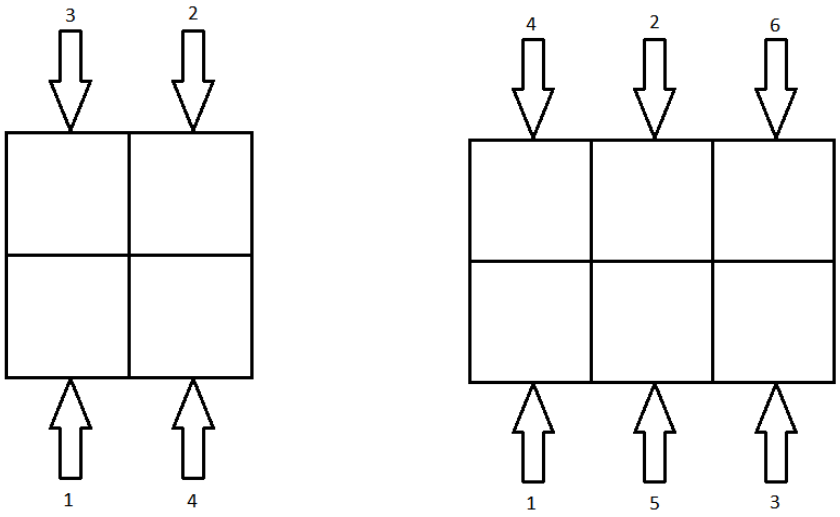

Figure 6.7 - Four and Six Burner Control Zone Firing Sequences

6.4 – LFM Pulse Firing 160 t/hr Results

The following results are for the same furnace condition as previous, except the simulation applied a pulse firing technique.

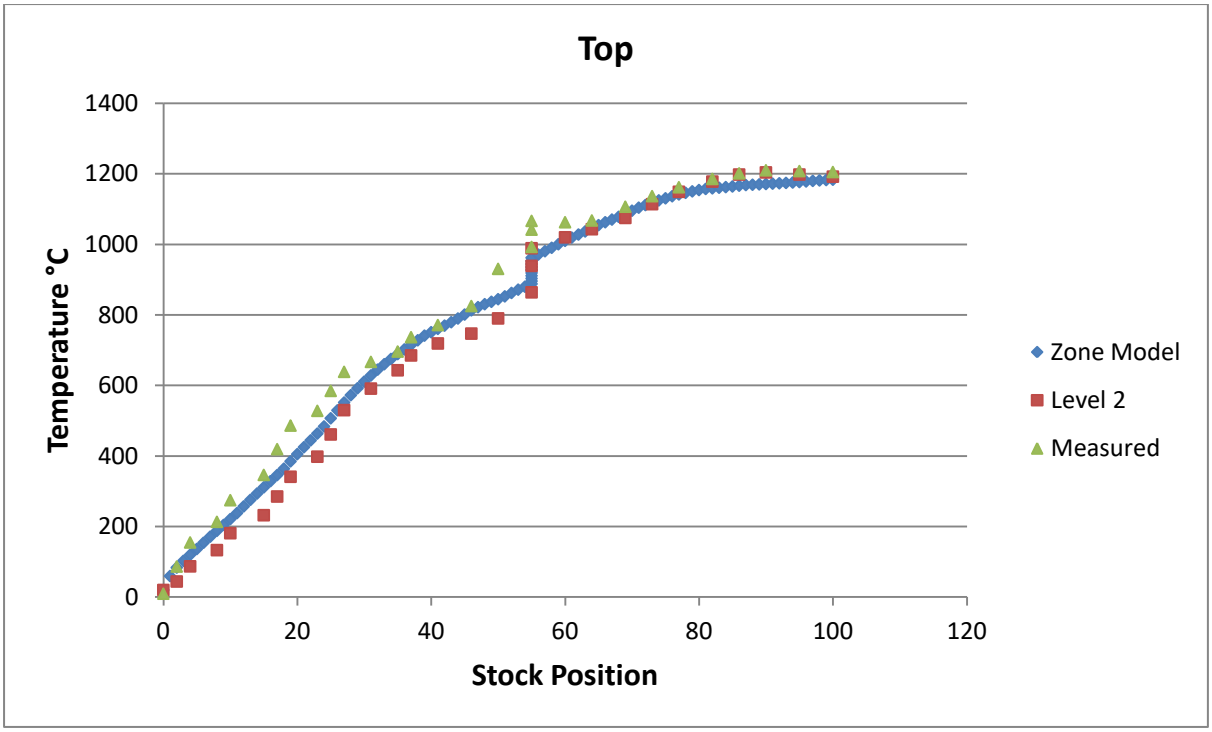
Top
Temperature °C
1400
1200
1000
800
600
400
200
0
0
20
40
60
80
100
120
Stock Position
Zone Model
Level 2
Measured

(a)

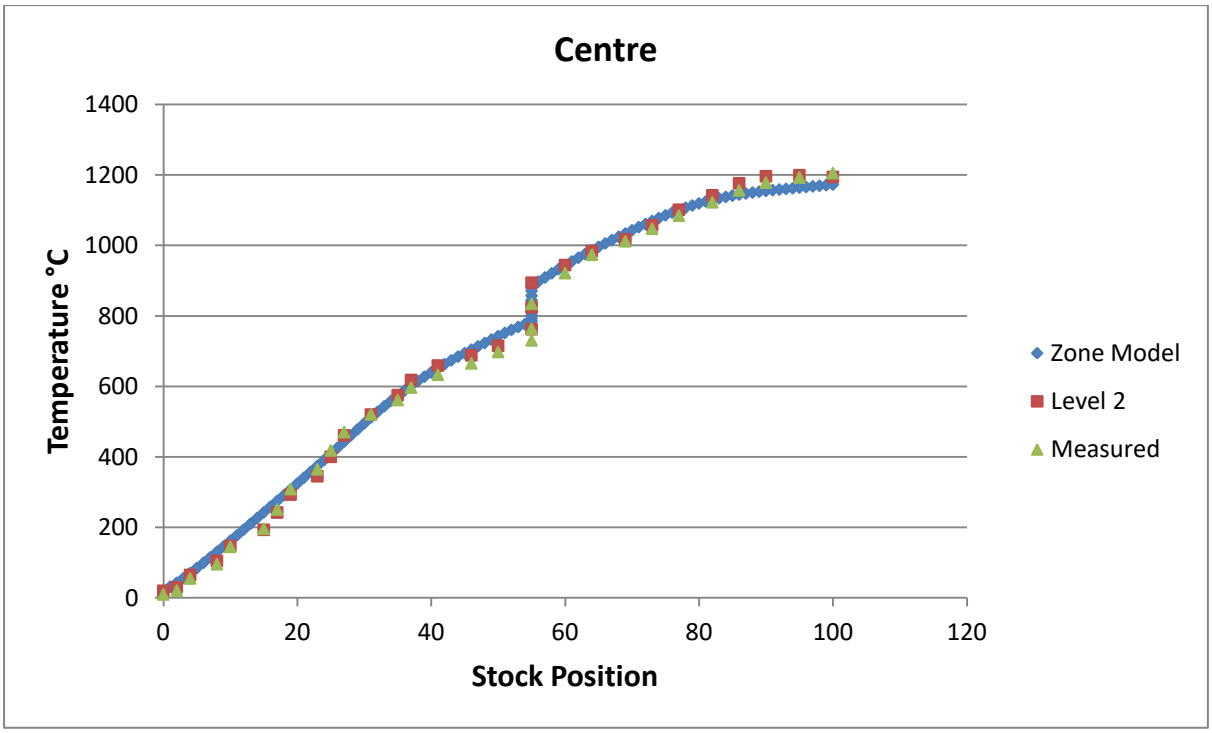
Centre
Temperature °C
1400
1200
1000
800
600
400
200
0
0
20
40
60
80
100
120
Stock Position
Zone Model
Level 2
Measured

(b)

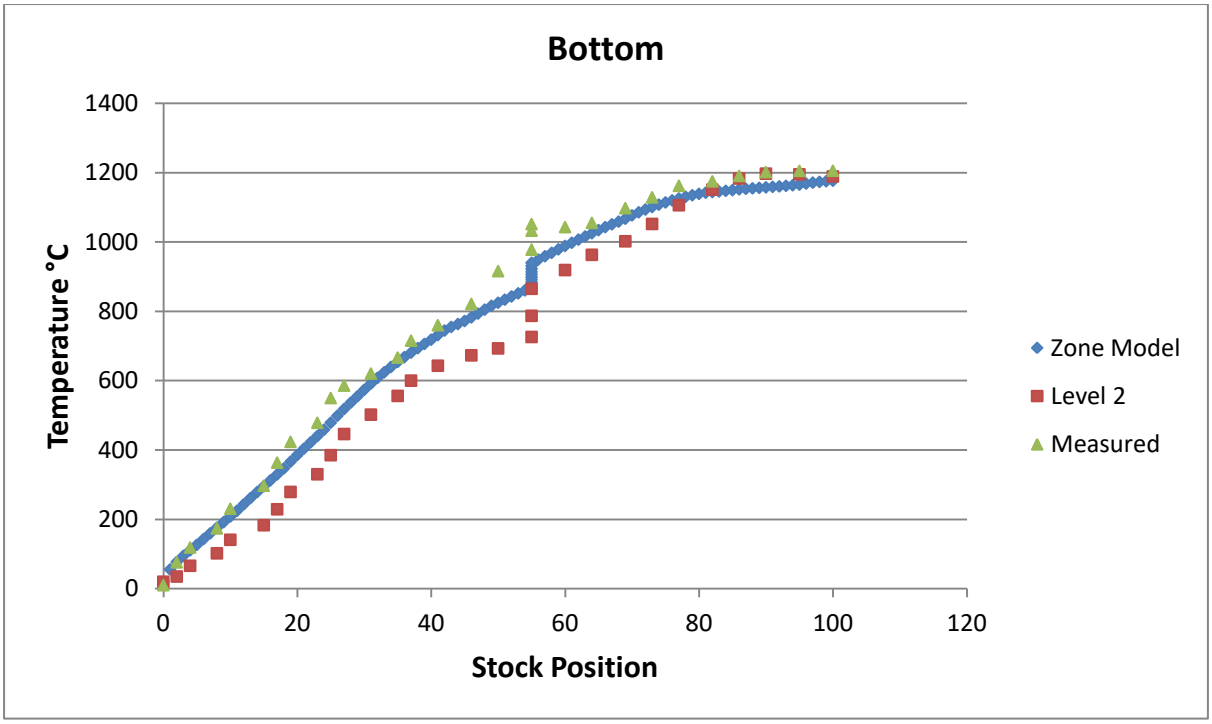

(c)

Figure 6.8 - LFM: 15 Minute Delay 20% Shadowing Pulse Fired - Temperature of (a) Top (b) Centre (c) Bottom Stock Nodes

Figure 6.8 shows a similar comparison to the measured data as did the results that did not utilise a pulse fired technique. The temperature profiles of the stock for both uniform and pulse firing are very similar. The temperature distribution within the stock at discharge was investigated (table 6.3)

	Uniform Firing	Pulse Firing
Minimum Node Temperature (K)	1438.98	1442.57
Maximum Node Temperature (K)	1455.63	1459.74
Temperature Difference (K)	16.66	17.18

Table 6.3 – Uniform and Pulse Firing Temperature Distribution Comparison

Table 6.3 shows that while the temperature difference is similar for both techniques, uniform firing gives slightly better temperature uniformity. The node temperatures for the measured data are unknown so this cannot be compared against.

6.5 – LFM 74 t/hr Results

Now that the simulation compares well with the experiment data for a 160 t/hr production rate, the model will now be validated by running a 74 t/hr simulation and comparing against TATA's level-2 model. The set point temperatures for this simulation which were found by trial and error to match the desired temperature profile are shown in table 6.3.

Control Zone	Set Point Temperature
1	800
2	800
3	850
4	850
5	950
6	950
7	1150
8	1150
9	1145
10	1145
11	1145

Table 6.4 - LFM - 74 t/hr Set Point Temperatures

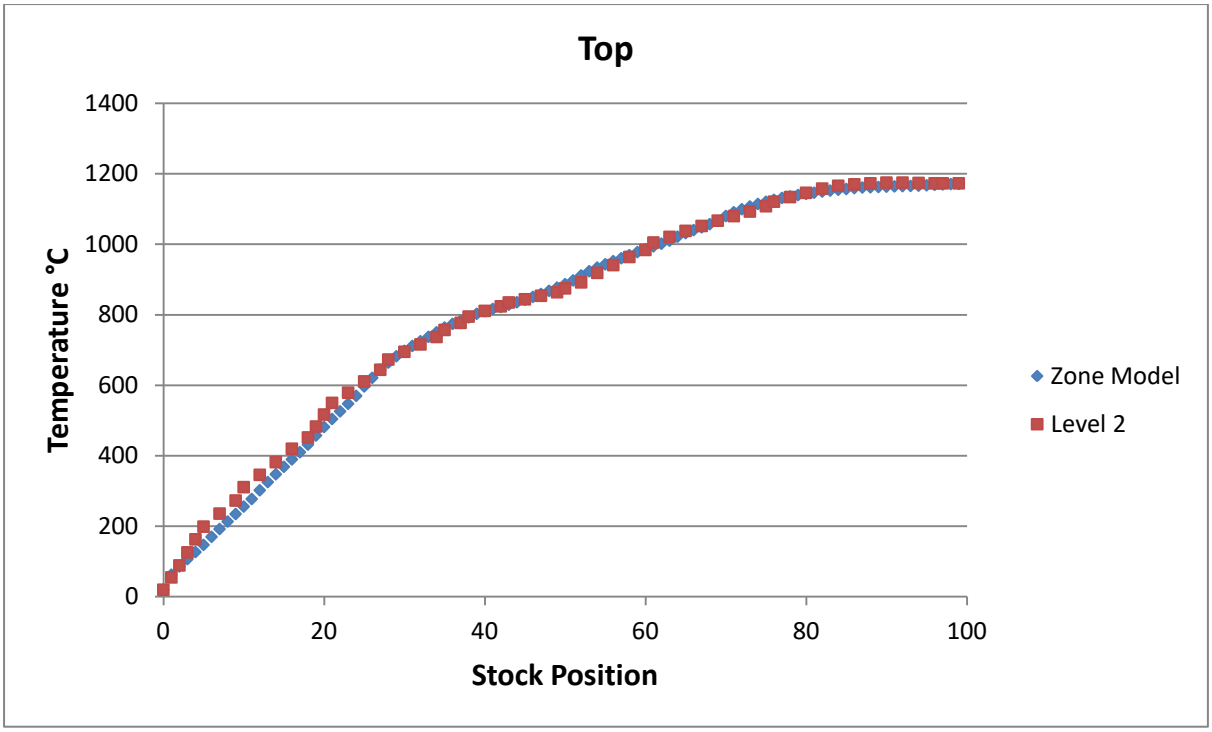
Top
1400
1200
1000
800
600
400
200
0
Temperature °C
0
20
40
60
80
100
Stock Position
Zone Model
Level 2

(a)

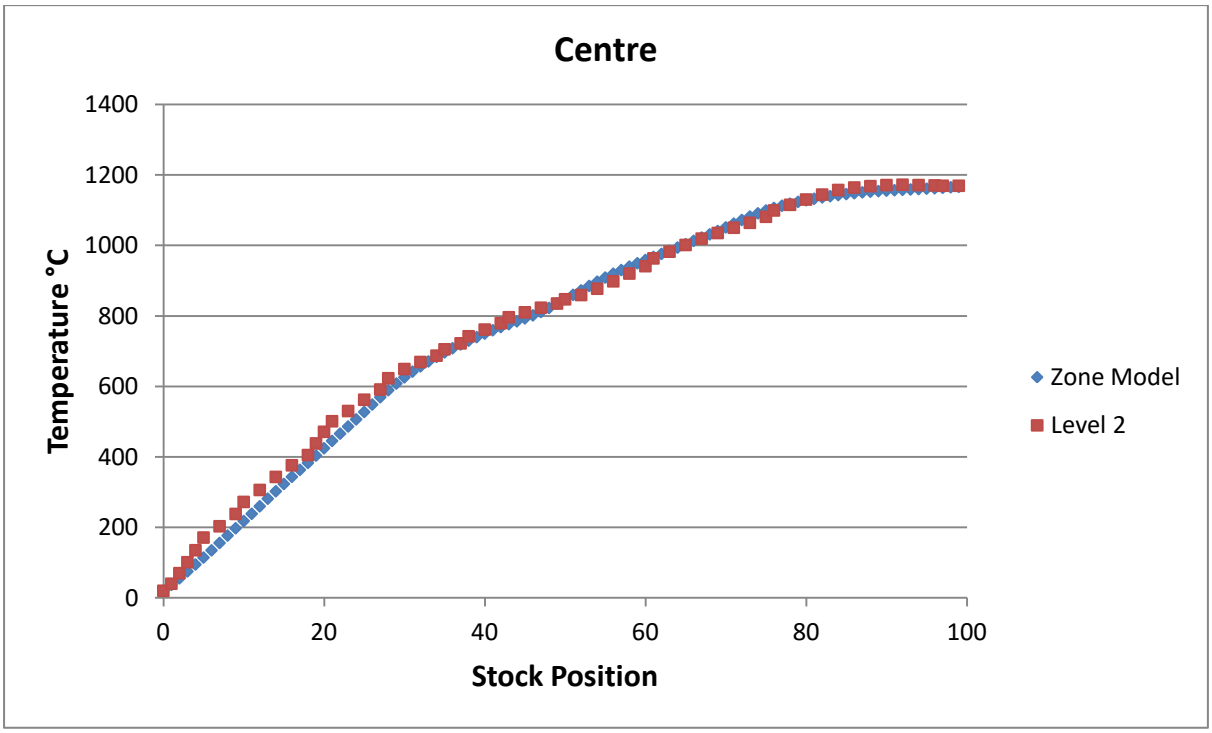
Centre
1400
1200
1000
800
600
400
200
0
Temperature °C
0
20
40
60
80
100
Stock Position
Zone Model
Level 2

(b)

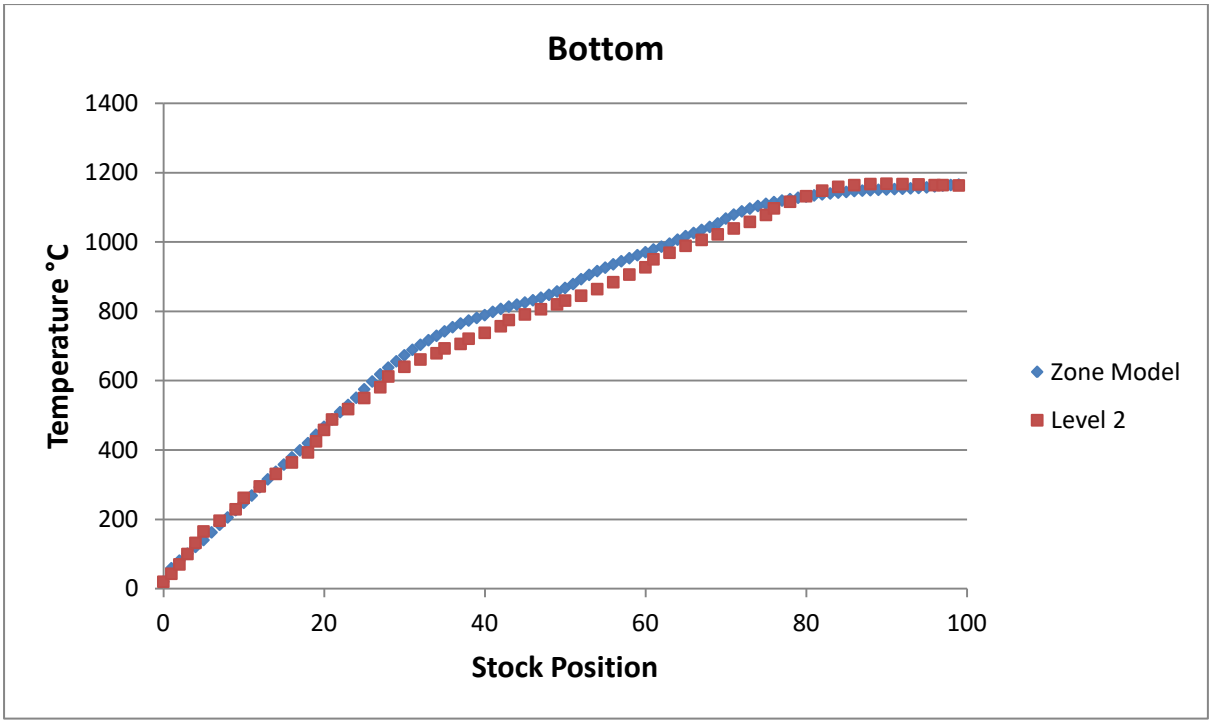

(c)

Figure 6.9 - 74 t/hr: Zone Model / Tata Level 2 Comparison - Temperature of (a) Top (b) Centre (c) Bottom Stock Nodes

Figure 6.9 shows close agreement with the data supplied by TATA Steel.

	Energy In (MW)	
QG_{net}	42.8	**Preheat (°C)**
Qa	4.5	360
Total	47.3	
	Energy Out (MW)	**%**
Qex	13.9	29.32
Qwc	10.6	22.37
Qwall	5.8	12.22
Qstock	17.1	36.09
Specific Fuel Consumption (GJ/Tonne)	2.08	
Maximum Stock Node Temperature Difference	9.98	

Table 6.5 - Energy Balance Output for 74 t/hr Simulation

The energy balance shown in table 6.5 shows that as this is a slower production rate, less thermal input is needed to reach the required discharge temperature. Also the maximum stock node temperature difference is less than that of the 160 t/hr production rate, meaning that the stock temperature is more uniform, which is expected as the stock is moving more slowly through the furnace.

Chapter 7 Conclusion

REFORM has been shown to calculate view factors with statistically acceptable error compared to analytical values when using a sufficiently large ray density. The percentage contribution of DEA between zone pairs very far apart is sufficiently small to ensure that the larger percentage differences in calculated view factors have a negligible effect on TEA calculations. Firing a larger bundle of rays reduces statistical error in the MCRT method. REFORM has also been shown to be as accurate as the previous program RADEX. However, when used to simulate the TATA Steel SRM furnace it allows for a much more realistic representation of the furnace enclosure, including calculations to individual obstacles as well as radiation interchange between the top and bottom sections of the furnace which are consistent with the fundamentals. Analysis of results demonstrates the usefulness of REFORM as a tool that can be extended to model fully radiation heat transfer.

The zone model simulation program has been validated by being shown to compare reasonably with the provided experiment data from a large-scale reheating furnace for different production rates and provided a closer estimation of the measured data than the level-2 models predictions. The model can also simulate delays, skid shadowing and water cooling losses. The inclusion of modelling the pulse fired behaviour of the burners provided no further improvement on the accuracy of the results. The model predicts the expected consequences of a lower production rates such as the decrease in thermal input and the increase in temperature uniformity and specific fuel consumption which is in agreement with behaviour seen in practice. The 3D model has a large computational overhead, while the LFM has a significantly reduced run time while not showing any detriment to accuracy.

This study has demonstrated the use of multi-dimensional mathematical zone models running under transient operating conditions that represents the entire furnace in one simulation and fully models each individual steel bloom. The REFORM program is highly flexible and can handle a range of geometries and combined with a transient zone model can be used for reheating process control.

Future Work

In the future it is expected that further improvements to the accuracy would be achieved by investigating the effect of stock ends heating. This is not usually considered as the ends have a relatively small surface area compared to their length. For such an investigation a 3D conduction model would be needed. Also, as the model relies on a plug flow assumption it might be found that a more accurate representation of the pulse firing flow is needed.

References

AMANATIDES, J. & WOO, A. (1987) A Fast Voxel Traversal Algorithm for Ray Tracing. *Proceedings of Eurographics*: 3-10.

ANTON, J. T. (2005). The influence of the space between the billets on the productivity of a continuous walking-beam furnace. *Applied Thermal Engineering* , 783-795.

ANTON, J., FRANCI, V. & TOMAŽ, K. (2007) Online simulation model of the slab-reheating process in a pusher-type furnace. *Applied Thermal Engineering*, 27(5-6): 1105-1114.

ANTON, J., TOMAŽ, K., BORUT, Z. (2005) The influence of the space between the billets on the productivity of a continuous walking-beam furnace, *Applied Thermal Engineering*, 25(5-6), 783-795.

BARR, P. V. (2003) Examining reheating furnace thermal response to mill delays. *Process Control and Optimization in Ferrous and Non Ferrous Industry*, USA.

BHARDWAJ, M. (2000) Calibration of Reheating Furnace Model Parameters at Hot Strip Mill, *TATA Search*: 57-60.

CHAKRABORTI, N., DEB, K. & JHA, A. (2000) A genetic algorithm based heat transfer analysis of a bloom re-heating furnace. *Steel research 71 No. 10*.

CHONG, Z. S., WILCOX, S. J., WARD, J. & BUTT, A. (1997) The development of a neural network controller for a chain grate, stoker-fired boiler. *4th European Conference on Industrial Furnaces and Boilers*, Portugal.

COELHO, P. J. (2001) Numerical simulation of radiative heat transfer from non-gray gases in three-dimensional enclosures. *Journal of Quantitative Spectroscopy & Radiative Transfer 74*.

CORREIA, S. (2001). *Development of improved mathematical models for the design and control of gas-fired furnaces.*

CORREIA, S. A. C., WARD, J. & SOUSA, J. L. V. A. (1999) The application of multi-zone thermal radiation models to investigate the energy efficiency of a metal reheating furnace under start-up conditions. *ASME*, Vol. AES- 39, Nashville, USA.

CORREIA, S. A. C., WARD, J. & SOUSA, J. L. V. A. (2000) Application of a multi-zone two-dimensional thermal radiation model for control of a metal reheating furnace under transient conditions. *3rd European Thermal Sciences Conference*.

CORREIA, S. A. C., WARD, J. & SOUSA, J. L. V. A. (2002) The application of a range of zone models to predict thethermal performance behaviour of a continuously operated metal reheating furnace. *6th European Conference on Industrial Furnaces and Boilers*, Estoril, Lisboa.

CORREIA, S.A.C. & WARD, J. (2002) The application of a two-dimensional zone model to the design and control of a continuously operated, gas-fired furnace. *Proceedings of the ASME International Mechanical Engineering Congress and Exposition*, New Orleans, LA, United States: 29-35.

CRANK, J. NICOLSON, P. (1947) A practical method for numerical evaluation of solutions of partial differential equations of the heat conduction type. *Proceedings of the Cambridge Philosophical Society*, 43 (1): 50-67.

DING, S., MANNAN, M.A. & POO, A.N. (2004) Oriented bounding box and octree based global interference detection in 5-axis machining of free-form surfaces. *Computer-Aided Design*, 36: 1281-1294.

DOCHERTY, P. & TUCKER, R. J. (1986) The influence of wall emissivity on furnace performance. *J. Inst. Energy*, pp. 35-37.

EASTOP, T. D. & MCCONKEY, A. (1993) Applied Thermodynamics for Engineering Technologists (5th Ed.). *Longman*, Singapore.

FITZGERALD, F. & SHERIDAN, A. T. (1969) The heating of a slab in a furnace. *Publication 123, I.S.I*, pp. 18-28.

FITZGERALD, F. & SHERIDAN, A. T. (1974) Prediction of temperature and heat transfer distribution in gas-fired pusher reheating furnaces. *J. Inst. Fuel*, 47, pp. 21-27.

FITZGERALD, F. (1969) Aspects of furnace design for hot working. *Publication 111, I.S.I*, pp. 18-28.

FRANCI, V., JAKILE, A., KOKALJ, T. & MATKO, D. (2008) A furnace control system for tracing reference reheating curves. *Steel Research International*, USA.

FRICKER, N., WARD, J., WILCOX, J., CHONG, A., TAN, C.K., TUCKER, R., GEORGE, E., VILLERMAUX, C. & FERLIN, T. (2009) Multimode modelling approach for NOx reduction on gas fired glass melters through flame/furnace matching. *Presented at 16th IFRF Members' Conference*, Boston, USA: 8-10.

GOUTIERE, V. LIU, F. & CHARETTE, A. (1999) An assessment of real-gas modelling in 2D enclosures. *Journal of Quantitative Spectroscopy & Radiative Transfer 64*.

HILDEBRAND, F. (1987) Introduction to Numerical Analysis. *Dover Publications*.

HOTTEL, H. C. & COHEN, E. S. (1958) Radiant heat exchange in a gas-filled enclosure: allowance for non-uniformity of gas temperature. *J. AIChE*, pp. 3-13.

HOTTEL, H. C. & SAROFIM, A. F. (1967) Radiative Transfer. *McGraw-Hill*, New York, USA.

HOWELL, J. R. (1997) The Monte Carlo Method in Radiative Heat Transfer. *Journal of Heat Transfer*: 547-560.

INCROPERA, F.P. & DE WITT, D.P. (1990) Introduction to Heat Transfer. *John Wiley & Sons*, Singapore.

JANG, Y. J. AND KIM, S. W. (2007) An Estimation of a Billet Temperature during Reheating Furnace Operation. *International Journal of Control, Automation and Systems*, Vol. 5, No. 1, pp. 43-50.

JENKINS, B. G. & MOLES, F. D. (1981) Modelling of heat transfer from a large enclosed flame in a rotary kiln. *Trans. IChemE*, vol 59, pp. 17-25.

JENKINS, J., TAN, C.K., WARD, J. & BROUGHTON, J. (2011a) Development of a three-dimensional mathematical model for real-time simulation of continuous reheating furnace operations. *Proceedings of AISTech The Iron and Steel Technology Conference and Exposition,* Indiana Convention Center, Indianapolis, USA.

JENKINS, J., TAN, C.K., WARD, J. & BROUGHTON, J. (2011b) An Improved Mathematical Model to Predict the Real Time Transient Performance of a Large Steel Reheating Furnace. *Proc. ASME International Mechanical Engineering Congress & Exposition*, Denver, Colorado, USA. Paper IMECE2011-636912011.

KREUZER, D. R. & WERNER, A. (2011) Implementation of Models for reheating processes in industrial furnaces. *Proceedings of the 8th International Modelica Conference*, 063:041

LATHAM, D. A., MCAULEY, K. B., PEPPLEY, B. A. & RAYBOLD, T. M. (2011) Mathematical modelling of an industrial steam-methane reformer for on-line deployment. *Fuel Processing Technology*: 1574-1586.

LAWSON, D. A. & ZIESLER, C. D. (1996) An accurate program for radiation modelling in the design of high-temperature furnaces. *Journal of Management Mathematics*, 7(2): 109-116.

LAWSON, D. A. (1991) RADEX User Guide. *Coventry University*.

LAWSON, D. A. (1995) An improved method for smoothing approximate exchange areas. *International Journal of Heat Mass Transfer*, 38(16): 3109-3110.

LEDEN, B. (1985) Mathematical Reheating Furnace Models in STEELTEMP. *Proceedings of the International Conference on Process Control and Energy Savings in Reheating Furnaces*, (2): 1-2.

LUCAS, S. (1997) RadCAD: Validation of a New Thermal Radiation Analyzer. *SAE Technical Paper*, 10.4271/972442.

MADSEN, E. E. (1994) STEELTEMP - A Program for Temperature Analysis in Steel Plants, *Journal of Materials Processing Technology*, 42(2): 187-195.

MALHOTRA, C. P. (2003) Comparison of control strategies for reheating furnaces. *Materials Science & Technology Conference*, Chicago, IL, USA: 137-148.

MODEST, M. F. (1991) The Weighted-Sum-of-Gray-Gases Model for Arbitary Solution Methods in Radiative Transfer. *Journal of Heat Transfer*, Vol. 113.

MOHAMMED, S. N. (1997) Investigating the effects of changes in furnace operation conditions using the well-stirred model. *Leonardo Electric Journal of Partices and Technologies*, pp. 99-108.

NOBLE, J. (1975). The zone method: explicit matrix relations for total exchange areas. *Heat and Mass Transfer*, 18(2): 261-269.

NORBERG, P. O. (1997) Challenges in the control of the reheating and annealing process. *Scandinavian Journal of Metallurgy*, 26(5): 206-214.

OMORI, T. (1990) Monte Carlo simulation of indoor radiant environment. *Intl. J. Num. Meth. Eng*, vol 30, pp. 615-627.

OMORI, T., NAGATA, T. & TANIGUCHI, H. (1991) Three-dimensional heat transfer analysis of a steel heating furnace. *7th Intl. Conf. on Numerical Methods in Thermal Problems*.

RHINE, J. M. & TUCKER, R. J. (1991) Modelling of Gas-Fired Furnaces and Boilers. *McGraw-Hill*, New York, USA.

ROSE, J., & COOPER, J. R. (1977). Technical Data on Fuel.

SALTER, F. M. & COSTICK, J. A. (1974) Mathematical model of the heat transfer within a reheating furnace. *J. Inst. Fuel*, pp. 3-19.

SAMBI, M. S. & TUCKER, R. J. (1983) Mathematical modelling of the thermal performance of furnaces operating under non-steady state conditions. *Proc. Intl Gas Resecrah Conf*, London.

SMITH, T. F. & SHEN, Z. H. (1981) Evaluation of coefficients for the weighted sum of grey gases model. *ASME, J. Heat Transfer*, pp. 602-608.

SOUSA, J. L. V. A., WARD, J., WALLIS, R. A. & LAWSON, D. A. (1996) Simulation and measurement of the transient performance of a gas-fired heat treatment furnace. *2nd European Thermal Science & 14th UIT National Heat Transfer Conf*, Rome, Italy.

STAALMAN, D. (2004) The Funnel Model for Accurate Slab Temperature in Reheating Furnaces. *La Revue de Métallurgie*, 101(6): 453-459.

STEWARD, F. R. & GURUZ, H. K. (1974) Mathematical simulation of an industrial boiler by the zone method of analysis. *In NH Afgan, JM Beer (eds.)*, Heat Transfer in Flames, John Wiley & Sons, New York.

STEWARD, F. R. & TENNANKORE, K. N. (1979) Towards a finite solution coupled with the zone method for radiative transfer for a cylindrical combustion chamber. *J. Inst. Energy*, pp. 107-114.

TAYLOR, P. B. AND FOSTER, P. J. (1974) The Total Emissivities of Luminous and Non-Luminous Flames. *Int. J. Heat Mass Transfer*, Vol. 17, pp. 1591-1650.

TRIVIC, D. N. (2004) Modeling of 3-D non-gray gases radiation by coupling the finite volume method with weighted sum of gray gases model. *International Journal of Heat and Mass Transfer 47*.

TRUELOVE, J. S. (1976) A mixed grey gas model for flame radiation. *UKAEA Report*, AERE-R-8494, Harwell.

TUCKER, R. J. & LORTON, R. (1984) Mathematical Modelling of Load-Recuperative Gas-Fired Furnaces. *Institution of Chemical Engineers Symposium Series,* 86: 1035-1046

TUCKER, R. J. & WARD, J. (1986) Use of a Monte-Carlo technique for determination of radiation exchange areas in long furnace models. *Proc. 8th International Heat Transfer Conf., San Francisco*, USA, (2): 391-396.

TUCKER, R. J. & WARD, J. (1990) Mathematical-modelling of heat-transfer in a gas-fired reheating furnace operating under non-steady state conditions. *9th International conf on Heat Transfer*, Jerusalem, Israel, (1-7): 221-226.

TUCKER, R. J. (1995) Advances in radiation transfer for gas-fired furnace design. *IMechE*, pp. 487-497.

TUCKER, R. J., WARD, J. & CORREIA, S. A. C. (2008) The effect of installing porous refractory panels on the transient start up performance of a gas-fired reheating furnace. *ASME, Intl. Mechanical Engineering Congress and Exposition*, Boston, USA.

VENTURINO, M. & RUBINIKER, P. (1995) Coupled Fluid Flow and Heat Transfer Analysis of Steel Reheat Furnaces. *Proceedings of 3rd European Conference on Industrial Furnaces and Boilers*.

VERCAMMEN, H. A. J. AND FROMENT, G. F. (1980) An Improved Zone Method using Monte Carlo Techniques for the Simulation of Radiation in Industrial Furnaces. *Int. J. Heat Mass Transfer*, Vol 23, pp. 329-337.

WALKER, J., Xue, S.-C. & Barton, G.W. (2010) Numerical Determination of Radiative View Factors Using Ray Tracing. *Journal of Heat Transfer*, 072702 (132): 1-6.

WARD, J., WILCOX, S. J. & PAYNE, R. (1999) Prediction of the thermal performance of a high temperature furnace using neural networks. *6th UK National Heat Transfer Conference*, Edinburgh.

WILD, D., MEURER, T. AND KUGI, A. (2009) Modelling and experimental model validation for a pusher-type reheating furnace. *Mathematical and Computer Modelling of Dynamical Systems*, Vol. 15, No. 3, 209-232.

WU, W., FENG, Y. AND ZHANG, X. (2007) Zonal method solution of radiative heat transfer in a one-dimensional long roller-hearth furnace in CSP. *Journal of University of Science and Technology*, Vol 14, No. 4, Beijing.

YAN, W., ZHANG, F. (2000) Mathematical Model Study on Billet Heating Furnace, *Industrial Furnace,* 22(2): 54-58.

YU, M. J., BAEK, S. W. & PARK, J. H. (2000) An extension of the weighted sum of gray gases non-gray gas radiation model to a two phase mixture of non-gray gas with particles. *International Journal of Heat and Mass Transfer 43*.

ZEEB, C.N. & BURNS, P.J. (1999) Performance Enhancements of Monte Carlo Particle Tracing Algorithms for Large, Arbitrary Geometries. *In proceedings of the 1999 ASME National Heat Transfer Conference,* Albuquerque, NM: 15-17.

ZONGYU, L., BARR, P. V. & BRIMACOMBE, J. K. (1987) Computer Simulation of the Slab Reheating Furnace. *Canadian Metallurgical Quarterly*. Vol. 27, No. 3, pp. 187-196.

Published Papers Developed From This Study

Matthew AD, Tan CK, Roach PA, Ward J, Broughton J, Heeley A, 2014. Calculation of the Radiative Heat-Exchange Areas in a Large-Scale Furnace with the Use of the Monte Carlo Method. Journal of Engineering Physics and Thermophysics, 87(3): 732-742.